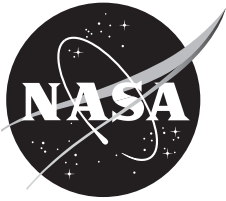


NASA/TM-2013-215983



Programmable Portable Guidance Display Users Manual

Gordon H. Hardy

Science Application International Corporation (SAIC)

Ames Research Center, Moffett Field, California

March 2013

The NASA STI Program Office . . . in Profile

Since its founding, NASA has been dedicated to the advancement of aeronautics and space science. The NASA Scientific and Technical Information (STI) Program Office plays a key part in helping NASA maintain this important role.

The NASA STI Program Office is operated by Langley Research Center, the Lead Center for NASA's scientific and technical information. The NASA STI Program Office provides access to the NASA STI Database, the largest collection of aeronautical and space science STI in the world. The Program Office is also NASA's institutional mechanism for disseminating the results of its research and development activities. These results are published by NASA in the NASA STI Report Series, which includes the following report types:

- **TECHNICAL PUBLICATION.** Reports of completed research or a major significant phase of research that present the results of NASA programs and include extensive data or theoretical analysis. Includes compilations of significant scientific and technical data and information deemed to be of continuing reference value. NASA's counterpart of peer-reviewed formal professional papers but has less stringent limitations on manuscript length and extent of graphic presentations.
- **TECHNICAL MEMORANDUM.** Scientific and technical findings that are preliminary or of specialized interest, e.g., quick release reports, working papers, and bibliographies that contain minimal annotation. Does not contain extensive analysis.
- **CONTRACTOR REPORT.** Scientific and technical findings by NASA-sponsored contractors and grantees.

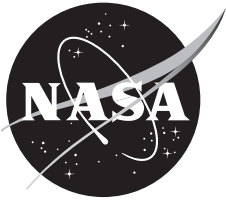
- **CONFERENCE PUBLICATION.** Collected papers from scientific and technical conferences, symposia, seminars, or other meetings sponsored or cosponsored by NASA.
- **SPECIAL PUBLICATION.** Scientific, technical, or historical information from NASA programs, projects, and missions, often concerned with subjects having substantial public interest.
- **TECHNICAL TRANSLATION.** English-language translations of foreign scientific and technical material pertinent to NASA's mission.

Specialized services that complement the STI Program Office's diverse offerings include creating custom thesauri, building customized databases, organizing and publishing research results . . . even providing videos.

For more information about the NASA STI Program Office, see the following:

- Access the NASA STI Program Home Page at <http://www.sti.nasa.gov>
- E-mail your question via the Internet to help@sti.nasa.gov
- Fax your question to the NASA Access Help Desk at (301) 621-0134
- Telephone the NASA Access Help Desk at (301) 621-0390
- Write to:
NASA Access Help Desk
NASA Center for AeroSpace Information
7115 Standard Drive
Hanover, MD 21076-1320

NASA/TM-2013-215983



Programmable Portable Guidance Display Users Manual

Gordon H. Hardy

Science Application International Corporation (SAIC)

Ames Research Center, Moffett Field, California

National Aeronautics and
Space Administration

Ames Research Center
Moffett Field, California 94035-1000

March 2013

Available from:

NASA Center for AeroSpace Information
7115 Standard Drive
Hanover, MD 21076-1320
(301) 621-0390

National Technical Information Service
5285 Port Royal Road
Springfield, VA 22161
(703) 487-4650

TABLE OF CONTENTS

List of Figures.....	v
List of Tables.....	v
Nomenclature.....	vi
1.0 Introduction.....	1
2.0 Lateral Navigation (LNAV) Algorithms.....	3
2.1 Example Two-Turn Approach.....	3
2.2 Input Required.....	4
2.3 Output Provided.....	5
3.0 Vertical Navigation (VNAV) Algorithms.....	7
3.1 VNAV with Continuous Flightpath Angle and Velocity Rate (Finite Rate of Change of Inceptor).....	7
3.2 VNAV with Discontinuous Velocity Rate (Step Change of Inceptor).....	12
4.0 Flightpath, Velocity, and Longitudinal Flight Director Display Algorithms.....	13
4.1 General.....	13
4.2 Vertical Flightpath Symbol, γ_{LQ}	17
4.3 Velocity Rate of Change Caret, $\Delta\dot{V}_Q$	18
4.4 Engine Model.....	19
4.5 Nominal Pitch, θ_N , and Thrust Lever Angle, δ_{TN} (or T_N).....	20
4.6 Flight Director.....	21
4.7 Mode Control and RNAV Capture.....	22
5.0 PPGD Simulink Model.....	23
6.0 PPGD Interfaces to the Aircraft (or Simulator) and to the Display.....	25
6.1 General.....	25
6.2 Aircraft (or Simulator) Interface.....	25
6.3 NAV Display Interface.....	26
6.4 PFD and HUD Display Interface.....	26
7.0 Simulink Model Data Requirements.....	29
7.1 General.....	29
7.2 LNAV Subsystem.....	29
7.3 Auto-Flap Subsystem.....	30
7.4 VNAV Subsystem.....	30
7.5 Quickened FP & Vel Rate Subsystem.....	31

TABLE OF CONTENTS (cont.)

7.6 MSP & RNAV CAP Subsystem.....	32
7.7 Flight Director and Leader Subsystem	33
7.8 NAV DOTS MATLAB Function Block.....	34
7.9 PFD and HUD Display Subsystem.....	34
Appendix A: LNAV Algorithm Derivations	37
Appendix B: VNAV Algorithm Derivations	39
Appendix C: Flightpath, Velocity, and Longitudinal Flight Director Display Derivations	47
References.....	51

LIST OF FIGURES

Figure 1.1. Programmable Portable Guidance Display.....	2
Figure 2.1. Example LNAV approach to SFO 28R.	3
Figure 3.1. Example VNAV for a tiltrotor.	8
Figure 3.2. Example γ/V diagram for a STOL vehicle.	9
Figure 4.1a. Pursuit display elements.	13
Figure 4.1b. Vertical pursuit display elements.....	14
Figure 4.1c. Leader perspective angles.	14
Figure 4.2. Pursuit display and pitch flight director configuration.	15
Figure 4.3. Blend of airspeed to ground speed.....	16
Figure 4.4. Flightpath control.....	17
Figure 4.5. Velocity rate control.	18
Figure 5.1. PPGD conceptual Simulink model.	23
Figure 5.2. PPGD input constants MATLAB m file.....	24
Figure B1. Altitude assumptions	39
Figure B2. Velocity assumptions.....	41

LIST OF TABLES

Table 3.1. VNAV Segment Endpoints.....	11
Table 3.2. Example CTR VNAV Segment Endpoints.....	12

NOMENCLATURE

Acronyms

CESTOL	cruise-efficient short take-off and landing
CTOL	conventional takeoff and landing
EFF FPA	effective flightpath angel
HSI	horizontal situation indicator
HUD	head-up display
LNAV	lateral navigation
MSL	mean sea level
NAV	navigation display
PFD	Primary Flight Display
PPGD	Programmable Portable Guidance Display
RASCAL	Rotorcraft Aircrew Systems Concepts Airborne Laboratory
RNAV	area navigation
TOGA	Take-Off/Go-Around
VNAV	vertical navigation
V/STOL	vertical/short takeoff and landing

Symbols

b	leader wingspan on the HUD or PFD,	deg
$curv$	LNAV path curvature (1/radius),	ft ⁻¹
Δh	vertical error from the VNAV path (positive up),	ft
\dot{h}	rate of climb,	fps
K_S	velocity scaling,	kt/deg
p_γ	vertical perspective of the leader,	deg
p_ϕ	roll angle of the leader,	deg
p_ψ	lateral perspective of the leader,	deg
v	velocity,	fps
v_A	true airspeed,	fps
v_e	equivalent airspeed,	fps
v_G	ground speed,	fps
\dot{v}_{GA}	component of rate of change of ground speed along the true airspeed	fps ²
v_L	limited ground speed,	fps
v_W	the magnitude of the wind vector,	fps
x	distance along the VNAV path, zero at the start,	ft
Δy	lateral error from the LNAV path (positive right),	ft
P	standard day atmospheric pressure,	psf
P_{2500}	standard day atmospheric pressure at 2500 feet,	psf
T_L	lateral time constant of the leader,	sec
T_V	vertical time constant of the leader,	sec
$T_{\gamma V}$	thrust from the γ/V diagram,	pct

NOMENCLATURE (cont.)

Symbols (cont.)

T_N	thrust from the γ/V diagram corrected for altitude,	pct
V	ground speed,	knots
\dot{V}	rate of change of ground speed,	kt/sec
\ddot{V}	rate of change of \dot{V} ,	kt/sec ²
"V"	true airspeed/ground speed input to the acceleration caret,	knots
V_a	true airspeed,	knots
V_{ac}	true airspeed command,	knots
ΔV_C	commanded change in velocity,	knots
$\Delta \dot{V}_{CF}$	commanded filtered rate of change of speed,	deg
$\Delta \dot{V}_e$	velocity rate error,	fps ²
ΔV_F	displayed gained and filtered velocity error,	deg
\dot{V}_F	filtered rate of change of speed,	deg
$\Delta \dot{V}_F$	filtered minus nominal rate of change of speed,	deg
V_G	ground speed,	knots
V_{GC}	commanded ground speed,	knots
V_{GX}	component of ground speed along the nominal LNAV path,	knots
\dot{V}_θ	steady-state rate of change of airspeed to a step change in pitch,	deg/deg
\dot{V}_T	steady-state rate of change of airspeed to a step change in throttle,	deg/pct
\dot{V}_N	nominal rate of change of true airspeed/ground speed,	deg
\dot{V}_Q	total rate of change of velocity,	deg
$\Delta \dot{V}_Q$	quicken rate of change of velocity w.r.t. the nominal value,	deg
α	angle of attack,	deg
χ	track angle,	deg
$\Delta \chi_l$	leader's track measured from the nominal track,	deg
$\Delta \chi_{LC}$	limited commanded change in track,	deg
δ_T	thrust lever angle,	pct
δ_{TN}	nominal thrust lever angle on the LNAV path,	pct
$\Delta \delta_T$	difference between thrust and nominal thrust lever angle,	pct
δ_{TC}	flight director thrust lever angle command,	deg
δ_{TFC}	fixed thrust lever command,	pct
$\delta_{\gamma V}$	thrust lever angle from the γ/V diagram,	pct
γ	inertial flightpath angle,	deg
γ_A	flightpath angle with respect to the air mass,	deg
$\Delta \gamma_l$	leader's vertical flightpath angle measured from the nominal,	deg
γ_L	limited vertical flightpath angle,	deg
γ_{LC}	limited commanded vertical flightpath angle,	deg
$\Delta \gamma_{LC}$	limited commanded change in the vertical flightpath angle,	deg
γ_{LQ}	limited quickened vertical flightpath angle,	deg
γ_θ	steady-state γ response of the vehicle to a step in pitch,	deg/deg
γ_T	steady-state γ response of the vehicle to a step in thrust lever angle,	deg/pct
γ_x	rate of change of γ with x ,	deg/ft

NOMENCLATURE (cont.)

Symbols (cont.)

θ	pitch angle,	deg
θ_N	nominal pitch angle on the VNAV path,	deg
$\Delta\theta$	the difference between pitch and nominal pitch angle,	deg
θ_C	the flight director pitch command,	deg
$\theta_{\gamma V}$	pitch angle from the γ/V diagram,	deg
σ	atmospheric density ratio	
τ_e	time constant for the linearized first-order engine model,	sec
τ_H	heave time constant of the approximate first-order vehicle model,	sec
τ_T	turbulence smoothing filter time constant,	sec
ω_F	speed filter natural frequency,	rps
ψ	vehicle heading,	deg
ψ_W	heading of the wind vector (positive with the wind),	deg
ψ_t	nominal track on the LNAV path,	deg
ζ_F	speed filter damping ratio	

PROGRAMMABLE PORTABLE GUIDANCE DISPLAY USERS MANUAL

Gordon H. Hardy

Ames Research Center¹

1.0 INTRODUCTION

This manual provides information on the MATLAB/Simulink[®] implementation of the NASA Ames Research Center's Programmable Portable Guidance Display (PPGD) that enables users to develop pursuit guidance and flight director displays for research applications. The PPGD system supplies complete outer-loop guidance for lateral and longitudinal control along complex flightpaths for all classes of vehicles. All phases of flight are included: Take-Off/Go-Around (TOGA); climb, cruise, and descending; decelerating; and turning approaches to a hover. The manual provides derivations of the PPGD algorithms to facilitate future modifications. A more complete description of the underlying concepts is available in reference 1. Questions concerning the PPGD system should be referred to the author.

Almost 30 years of research on pursuit displays at the NASA Ames Research Center and the application of a pursuit display to a civil tiltrotor aircraft during the CTR-10 simulation at Ames during 2001 are discussed in reference 1. The work in that endeavor used the prior research to develop an "inverse" flight director to reduce pilot workload during the transition from the front-side (thrust for speed control) to back-side (pitch for speed control) configuration while preserving the advantages of the basic pursuit displays. Piloted control of this class of vehicle is challenging, particularly for the transition from the cruise front side to the final approach and landing back-side configuration. It is especially challenging for a precision descending, decelerating, turning, and time-constrained approach. Figure 1.1 shows the Primary Flight Display (PFD) driven by the PPGD system algorithms as used in the Rotorcraft Aircrew Systems Concepts Airborne Laboratory (RASCAL) Black Hawk helicopter application (ref. 2). For the Black Hawk helicopter application, no head-up display (HUD) was used, and this display format was presented on the head-down PFD. It includes the pursuit guidance and the "inverse" flight director developed during the civil tiltrotor work.

The basic elements of this display have been used in many previous NASA Ames vertical/short takeoff and landing (V/STOL) flight and simulation programs (refs. 3–8), and they have demonstrated the advantage of pursuit displays in combining situational awareness with command information. Both PFD and HUD implementations have been used.

¹ Science Application International Corporation (SAIC), Ames Research Center, Moffett Field, CA 94035-0001.

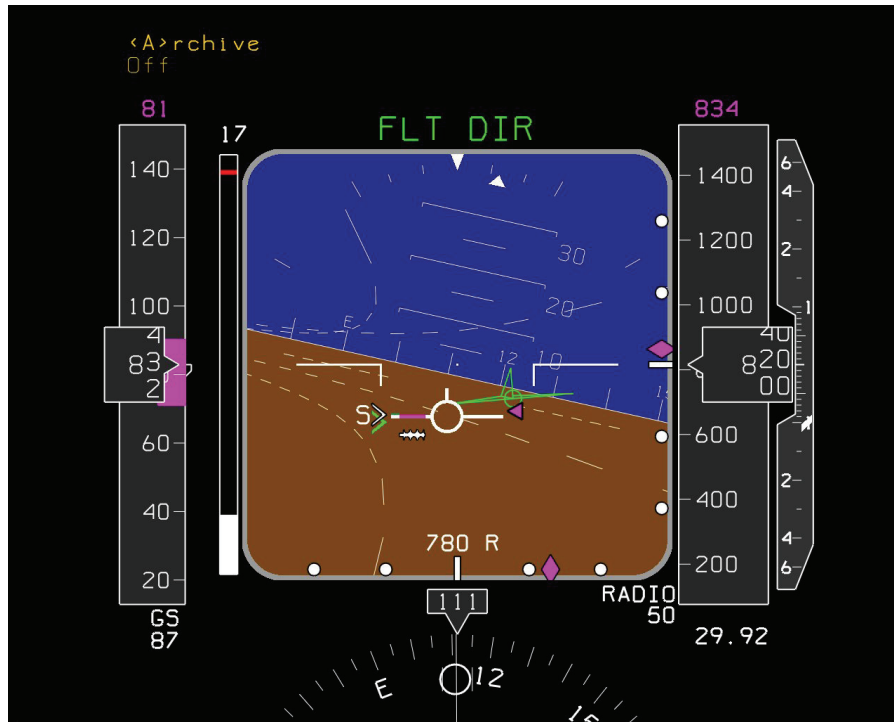


Figure 1.1. Programmable Portable Guidance Display.

In figure 1.1, the white flightpath symbol (circle with wings and tail) is shown near the center of the display; it is similar to that used for several operational HUDs. The essence of pursuit guidance is to place the flightpath on the leader, the green perspective delta wing airplane symbol in figure 1.1. This placement causes the vertical and lateral position errors to converge on the desired path exponentially with a time constant equal to the distance the leader is ahead of ownship. The leader is driven with scaled position errors and therefore combines command and situational information in a single flightpath-centered symbol, thereby minimizing the problem of concentrating on command (typically a flight director) and ignoring situational (raw data) information. The “Inverse” flight director pitch command is the magenta diamond off the right wing of the flightpath symbol and is referenced to the wing tip showing a small “pitch-up” command. The power (throttle, collective) command is the “handle” in the left wing; it is referenced to the wing and is showing an “add-power” command. The symbols are described in detail in section 4.0.

Sections 2.0 through 4.0 provide the algorithms used in the PPGD Simulink model given in section 5.0. Section 6.0 describes the input variables needed for the Simulink model from an aircraft or a simulator and the outputs to the displays. Section 7.0 describes the data required for the Simulink model. The appendices give derivations of the algorithms in sections 2.0 through 4.0.

2.0 LATERAL NAVIGATION (LNAV) ALGORITHMS

2.1 Example Two-Turn Approach

The example lateral navigation (LNAV) path shown in figure 2.1 is an approach to runway 28R at San Francisco International Airport. This example has the following LNAV segments:

- (1) Short straight leg between waypoint nm2 (n minus 2) and waypoint nm 1
- (2) 90-degree left turn to a downwind leg
- (3) Downwind leg
- (4) Tight 180-degree right base turn
- (5) Short final leg

The LNAV is potentially a path with n turns to a runway. The turns are constant-radius arc legs. They are joined by great-circle legs. For the example shown in figure 2.1, and in the present Simulink code, only two turns are available. Leg segment numbers are shown in the figure. The Simulink code is set up such that additional turns can be easily added. The algorithms for the spherical Earth great-circle legs are from reference 9. The algorithms for the turns assume flat Earth

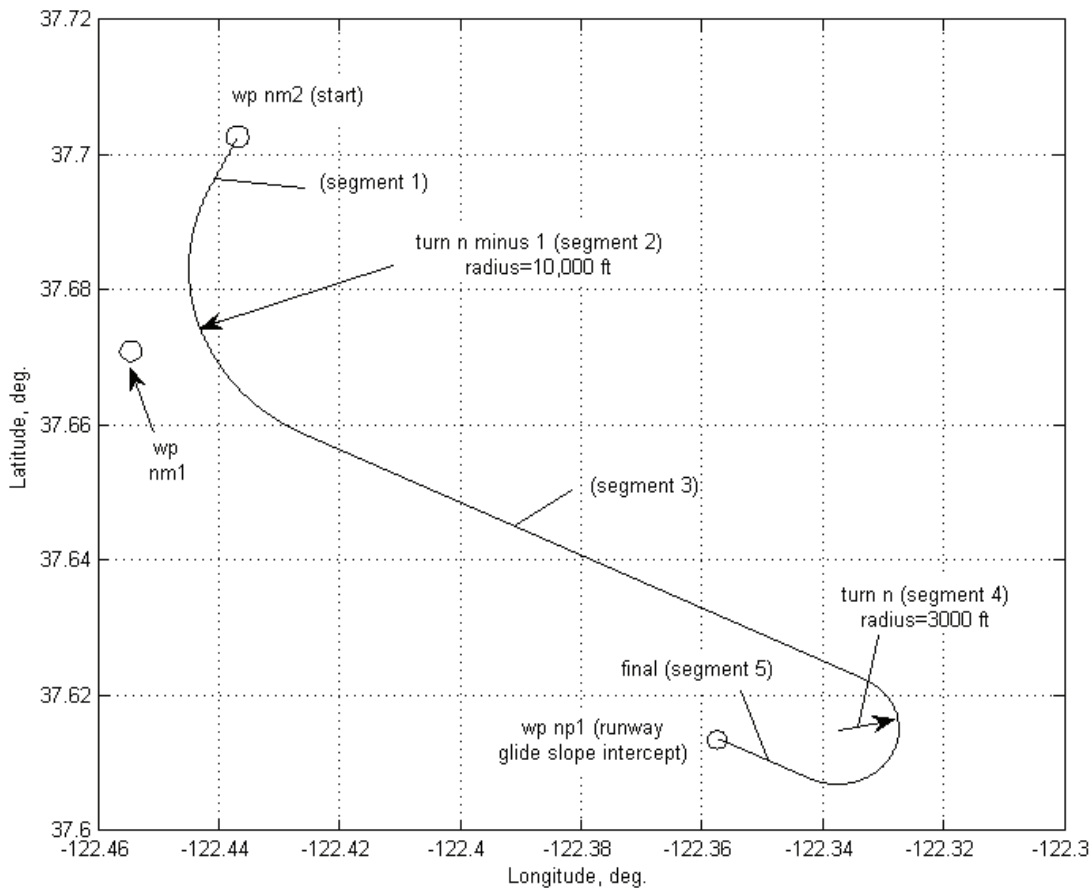


Figure 2.1. Example LNAV approach to SFO 28R.

approximations. The turn radii should therefore be kept reasonably small (maximum less than a few miles). The final turn is defined by joining the final leg at a specified distance from the runway glide-slope intercept and joining the great-circle downwind leg from waypoint nm1 (n minus 1). In the present code the size of the final turn must be kept less than 185 degrees to provide some tolerance for the turn from the downwind leg to the final leg. The location of the turn center at waypoint nm1 is defined by fairing the turn into the inbound and outbound great-circle legs. The code has been tested only for turns less than 135 degrees. For turns greater than about 135 degrees, fly-over waypoints would normally be used. No provision for fly-over waypoints is included in the code.

Since the turns use constant-radius arcs, there is a discontinuity in the heading rate entering and leaving the turn. Turn anticipation is provided to alleviate the need for step changes in bank angle.

Input and output parameters for guidance and control to follow the path and for display are discussed in the following sections.

2.2 Input Required

- lat_np1_deg waypoint np1 (n plus 1) latitude. This waypoint is nominally the glide-slope intercept point on the runway, deg
- lon_np1_deg waypoint np1 longitude, deg
- df final leg length; it is the length of the straight-in final approach after the final turn, n, feet
- psi_rw_deg the heading of the final leg (nominally runway heading), deg
- dir the direction of the final turn, 1 for a right turn and 0 for a left turn,
- rn_ft the radius of the final turn, feet
- lat_nm1_deg waypoint nm1 (n minus 1) latitude, deg
- lon_nm1_deg waypoint nm1 longitude, deg
- rnm1_ft the radius of turn at waypoint nm1, feet
- lat_nm2_deg waypoint nm2 (n minus 2) latitude, deg
- lon_nm2_deg waypoint nm2 longitude, deg
- initial_seg initial segment on the path. Each leg and each turn is a segment. For the example in figure 2.1 there are five segments, numbered 1–5. initial_seg is the segment number at the initial condition of the planned approach.
- k_bank_lead specifies how much turn anticipation is accomplished before the next segment. Turn anticipation assumes a constant roll rate to a roll angle based on the nominal turn radius and the present ground speed.
- lead_phidot leader's roll rate for turn anticipation, deg/sec

A MATLAB m function is provided in section 5.0 to convert the waypoint locations in runway coordinates into latitude and longitude assuming a flat Earth, if desired.

2.3 Output Provided

- `twocir_ye` lateral error measured perpendicular to the path, positive right, feet
- `twocir_psit` heading of the tangent to the path at the perpendicular point, feet
- `twocir_dist` distance along the path from the perpendicular point to waypoint `np1`, feet
- `dist_ngate` distance to the next segment on the path; this variable is used for turn anticipation, feet
- `iseg` number of the current segment, 1–5
- `persp_bank` bank angle command for turn anticipation, deg
- `k_trk` reduces the track command gain during turn anticipation

In addition to these variables the endpoints of the great-circle segments, the location of the start and end of the turn arcs, the arc lengths, and the arc centers are output to enable drawing the LNAV path on a NAV display if desired.

3.0 VERTICAL NAVIGATION (VNAV) ALGORITHMS

3.1 VNAV with Continuous Flightpath Angle and Velocity Rate (Finite Rate of Change of Inceptor)

3.1.1 Example for a Tiltrotor

Figure 3.1 shows an example vertical navigation (VNAV) path for a tilt rotor. This example has the following VNAV segments as shown in the first plot of figure 3.1:

- (1) Shallow climb, acceleration to climb speed
- (2) Steep climb, climb speed
- (3) Level acceleration to cruise speed
- (4) Level, constant cruise speed
- (5) Shallow descent at cruise speed
- (6) Shallow descent decelerating to the initial speed on final
- (7) Steep final approach with slow deceleration to touchdown speed

This example assumes a constrained path for climb. An alternate climb would use a fixed power setting with constant speed on an unconstrained vertical path.

The finite continuous velocity rate (finite slope) in velocity of this VNAV is seen in the velocity rate (fourth plot of fig. 3.1), which has no discontinuities.

3.1.2 Assumptions for This VNAV

- (1) Constant angle, γ , segments with short constant rate of change of γ with distance, γ_x , transitions between segments
- (2) Constant velocity segments or constant rate of change of velocity, \dot{V} , segments with short constant \dot{V} transitions between segments
- (3) The sum of velocity rate, \dot{V} , and the flightpath angle, γ , (effective flightpath angle (EFF FPA) in fig. 3.1) is continuous. This number provides the finite rate of change of inceptor characteristic.
- (4) The EFF FPA is consistent with the flightpath angle/speed envelope limits of the vehicle as determined from the γ/V diagrams (section 3.1.3) and is shown in figure 3.1.

3.1.3 Flightpath Angle/Speed Characteristics, γ/V

Figure 3.2 shows an example γ/V diagram for a STOL vehicle in the takeoff configuration. It shows the steady-state trimmed γ/V capability for various throttle positions as a fraction of full throttle. Also shown are lines of constant pitch angle, theta. The two circles at 160 knots correspond to the example that follows.

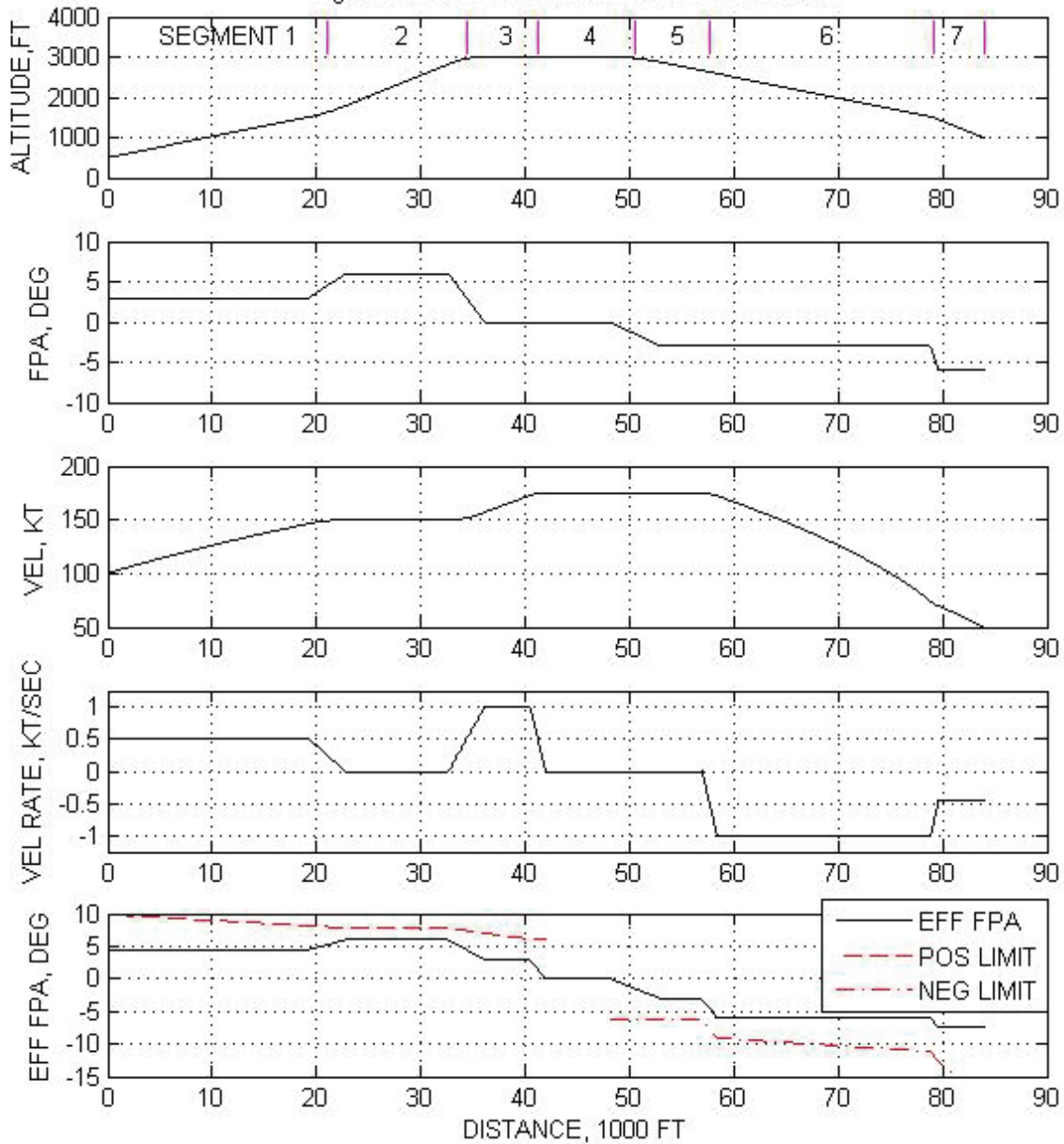


Figure 3.1. Example VNAV for a tiltrotor.

The equation of motion along the flightpath is:

$$\sum F_x - W \sin \gamma = m\dot{v} \tag{3.1}$$

where $\sum F_x$ is the sum of the external forces (thrust, drag, etc.) along the flightpath. Eq. (3.1) can be rewritten:

$$\frac{\sum F_x}{W} = \frac{\dot{v}}{g} + \sin \gamma$$

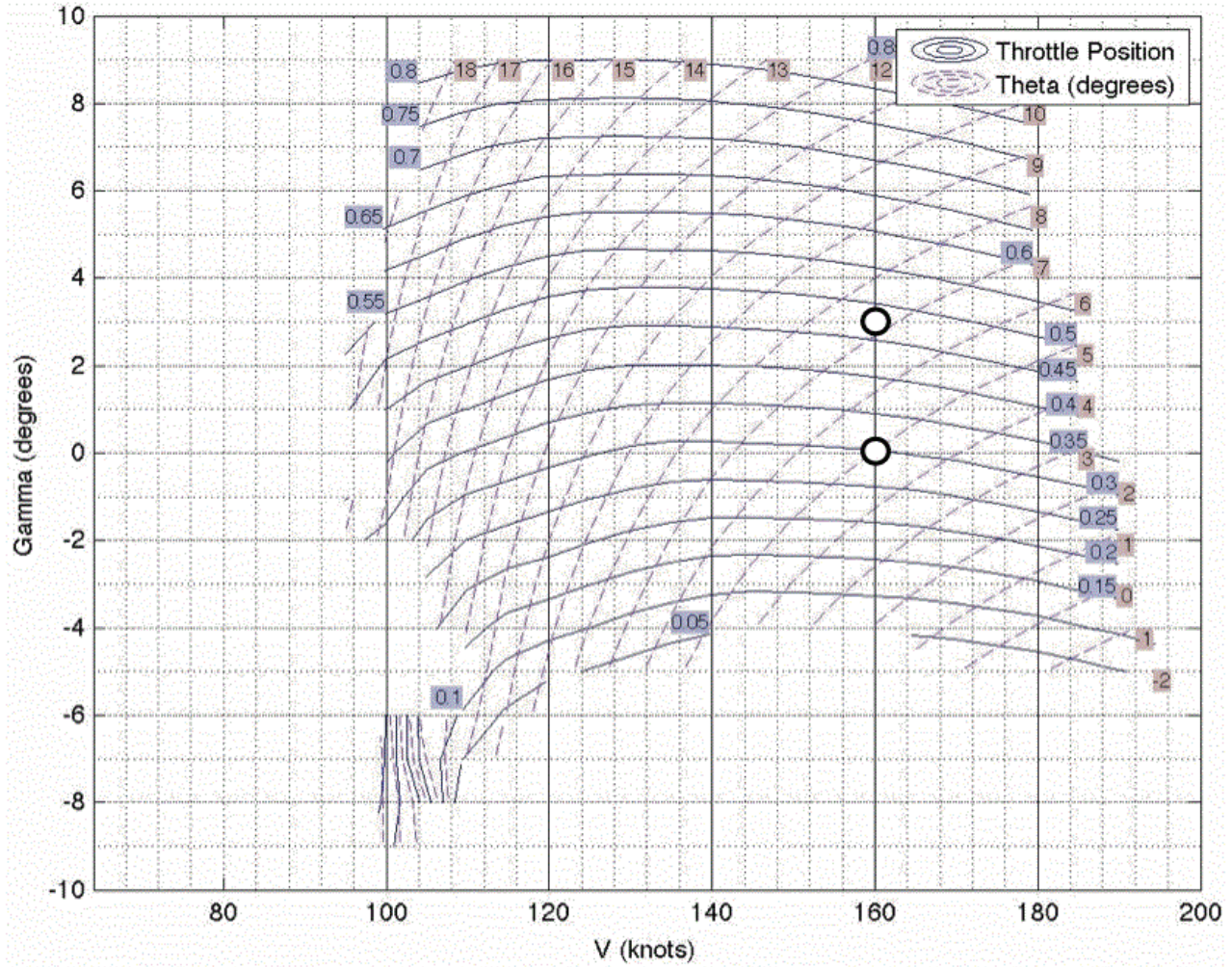


Figure 3.2. Example γ/V diagram for a STOL vehicle.

Assuming γ small and in degrees, this equation becomes:

$$\frac{180 \sum F_x}{\pi W} = \frac{180(1.69) \dot{V}}{\pi g} + \gamma \approx 3.0 \dot{V} + \gamma \quad (3.2)$$

where \dot{V} is in knots/second. For a given vehicle configuration (constant flaps, gear, throttle, α , V , etc.) the left side of the equation will be constant, and from Eq. (3.2) we can trade γ for \dot{V} on the γ/V diagrams. For example, from figure 3.2 we see that we can either climb at 3 degrees at a constant 160 knots with a throttle setting of 0.475 (right side of Eq. (3.2) equals 3) or we can accelerate at 1 knot/second at $\gamma = 0$ (right side of Eq. (3.2) also equals 3). For $\gamma = 3$, $\theta = 7.2$ while for $\gamma = 0$, θ would equal 4.2 degrees to keep α constant.

The last variable, EFF FPA, plotted in figure 3.1, is the right side of Eq. (3.2). This variable (for the planned VNAV profile) must have values consistent with the maximum and minimum values (color red in the figure) from the γ/V diagrams for the particular vehicle. Because some margin for control

must also be provided, a trade-off between the planned VNAV profile and the γ/V envelope limit values for each vehicle configuration is required.

3.1.4 VNAV Real-Time Calculations

For the flight director (section 4.6) we need target values for $\gamma(x)$, $h(x)$, $\dot{V}(x)$, and $V(x)$. From appendix B:

$$\Delta x = x - x_j$$

where the subscript j refers to the segment transition points along the VNAV path.

Altitude:

$$\gamma(x) = \gamma_j + \gamma_x(\Delta x) \quad (3.3)$$

$$h(x) = h_j + \left(\frac{\gamma_j + \gamma}{2}\right)(\Delta x) \quad (3.4)$$

Velocity:

for $\ddot{V} \neq 0$:

$$a = \frac{6V_j}{\ddot{V}} - 3\left(\frac{\dot{V}_j}{\ddot{V}}\right)^2$$

$$b = 2\left(\frac{\dot{V}_j}{\ddot{V}}\right)^3 - 6\left(\frac{\dot{V}_j V_j}{\ddot{V}^2}\right) - \frac{6}{1.69}\left(\frac{\Delta x}{\ddot{V}}\right) \quad (3.6)$$

for $\ddot{V} > 0$:

$$\Delta t(x) = -\frac{\dot{V}_j}{\ddot{V}} + \left(-\frac{b}{2} + SR\right)^{1/3} + \left(-\frac{b}{2} - SR\right)^{1/3} \quad (3.7)$$

where:

$$SR = \left(\frac{b^2}{4} + \frac{a^3}{27}\right)^{1/2}$$

for $\ddot{V} < 0$:

$$\Delta t(x) = -\frac{\dot{V}_j}{\ddot{V}} + 2\left(\frac{-a}{3}\right)^{1/2} \cos\left(\frac{\phi}{3} + \frac{4\pi}{3}\right) \quad (3.8)$$

where:

$$\phi = \cos^{-1}\left[\frac{b/2}{\sqrt{\frac{(-a)^3}{27}}}\right]$$

Then:

$$\dot{V}(x) = \dot{V}_j + \ddot{V}(\Delta t) \quad (3.9)$$

$$V(x) = V_j + \dot{V}_j(\Delta t) + \frac{\ddot{V}}{2}(\Delta t)^2 \quad (3.10)$$

for $\ddot{V} \equiv 0$, $\dot{V} = \text{constant}$:

$$\dot{V}(x) = \dot{V}_j \quad (3.11)$$

$$V(x) = \sqrt{V_j^2 + \frac{2\dot{V}_j(\Delta x)}{1.69}} \quad (3.12)$$

where:

x	ground distance along the flightpath, zero at the start,	ft
γ	inertial flightpath angle,	deg
γ_x	rate of change of γ with x ,	deg/ft
V	ground speed,	knots
\dot{V}	rate of change of ground speed,	kt/sec
\ddot{V}	rate of change of \dot{V} ,	kt/sec ²

Equations (3.3) through (3.12) give the necessary relations for calculating the flight director real-time target values during segments or transitions between segments. These equations were used to generate figure 3.1 using the example data in table 3.2.

Table 3.1 gives a format for tabulating the beginning values, j , for each segment or transition between segments and the rate of change of flightpath angle with distance, γ_x , and the rate of change of acceleration, \ddot{V} , during the segment transitions. Table 3.2 gives values for the example tilt rotor VNAV profile in figure 3.1. The values in table 3.2 were calculated using the algorithms in appendix B.

TABLE 3.1. VNAV SEGMENT ENDPOINTS

DESCRIPTION	WPT	ALTITUDE						VELOCITY		
		Δx FEET	x_j FEET	Δh FEET	h_j FEET	γ_j DEG	$\gamma_x \times 10^4$ DEG/FT	V_j KNOTS	\dot{V}_j KNOTS/SEC	$\ddot{V}_j \times 10^2$ KT/SEC ²
SEG 1: CLIMB, ACCEL										
SEG 1 TO 2 TRANSITION										
SEG 2: CLIMB										
SEG 2 TO 3 TRANSITION										
SEG 3: ACCEL										
SEG 3 TO 4 TRANSITION										
SEG 4: CRUISE										
SEG 4 TO 5 TRANSITION										
SEG 5: DESCEND										
SEG 5 TO 6 TRANSITION										
SEG 6: DESCEND, DECEL										
SEG 6 TO 7 TRANSITION										
SEG 7: DESCEND, DECEL										

NOTES:

TABLE 3.2. EXAMPLE CTR VNAV SEGMENT ENDPOINTS

DESCRIPTION	WPT	Δx FEET	x_j FEET	ALTITUDE				VELOCITY		
				Δh FEET	h_j FEET	γ_j DEG	$\gamma_x \cdot 10^4$ DEG/FT	V_j KNOTS	\dot{V}_j KNOTS/SEC	$\ddot{V}_x \cdot 10^2$ KT/SEC^2
	1		0		500	3		100	0.5	
SEG 1: CLIMB, ACCEL		19371		1015			0			0
	2		19371		1515	3		146.5	0.5	
SEG 1 TO 2 TRANSITION		3483		274			8.613			-3.6109
	3		22854		1789	6		150	0	
SEG 2: CLIMB		9790		1029			0			0
	4		32644		2818	6		150	0	
SEG 2 TO 3 TRANSITION		3483		182			-17.23			7.3873
	5		36127		3000	0		156.8	1	
SEG 3: ACCEL		4369		0			0			0
	6		40496		3000	0		172.5	1	
SEG 3 TO 4 TRANSITION		1472		0			0			-20
	7		41968		3000	0		175	0	
SEG 4: CRUISE		H -77718		0			0			0
	8		H -35750		3000	0		175	0	
SEG 4 TO 5 TRANSITION		4741		-124			-6.3280			0
	9		H -31009		2876	-3		175	0	
SEG 5: DESCEND		3959		-208			0			0
	10		H -27050		2668	-3		175	0	
SEG 5 TO 6 TRANSITION		1472		-77			0			-20
	11		H -25578		2591	-3		172.5	-1	
SEG 6: DESCEND, DECEL		20441		-1071			0			0
	12		H -5137		1520	-3		74.6	-1	
SEG 6 TO 7 TRANSITION		759		-60			-39.53			8.6141
	13		H -4378		1460	-6		70	-0.463	
SEG 7: DESCEND, DECEL		4378		-460			0			0
	14		H		1000	-6		50	-0.463	

NOTES: 1. H is total distance. Let H=84,000 feet

3.2 VNAV with Discontinuous Velocity Rate (Step Change of Inceptor)

Equations (3.3), (3.4), (3.11), and (3.12) are used for the simplified VNAV with step changes in the inceptor (power or pitch).

4.0 FLIGHTPATH, VELOCITY, AND LONGITUDINAL FLIGHT DIRECTOR DISPLAY ALGORITHMS

4.1 General

Figure 4.1a shows the elements of the pursuit displays. The details are discussed in reference 1. This section concentrates on the vertical part of the flightpath display, velocity control, and the longitudinal flight director. The drive signals for the leader symbol are given in figures 4.1a and 4.1b. For lateral path control, the pilot controls the flightpath symbol (actual track) laterally onto the leader symbol using bank angle. For vertical path control he uses quickened flightpath, γ_{LQ} , which is discussed in section 4.2. The velocity error tape (ΔV_F), the rate of change of nominal velocity (\dot{V}_N), and the rate of change of velocity with respect to the nominal value ($\Delta \dot{V}_Q$) on the left wing of the flightpath symbol are discussed in section 4.3. Section 4.6 discusses the flight director, and section 4.7 mode control. Sections 4.4 and 4.5 discuss details used in the other sections.

The flightpath symbol is limited to about 90% of the display area, and the leader symbol is then driven with respect to the flightpath and is limited to about 95% of the display area. This setup provides accurate guidance even if the display elements are limited. The symbols blink when limited.

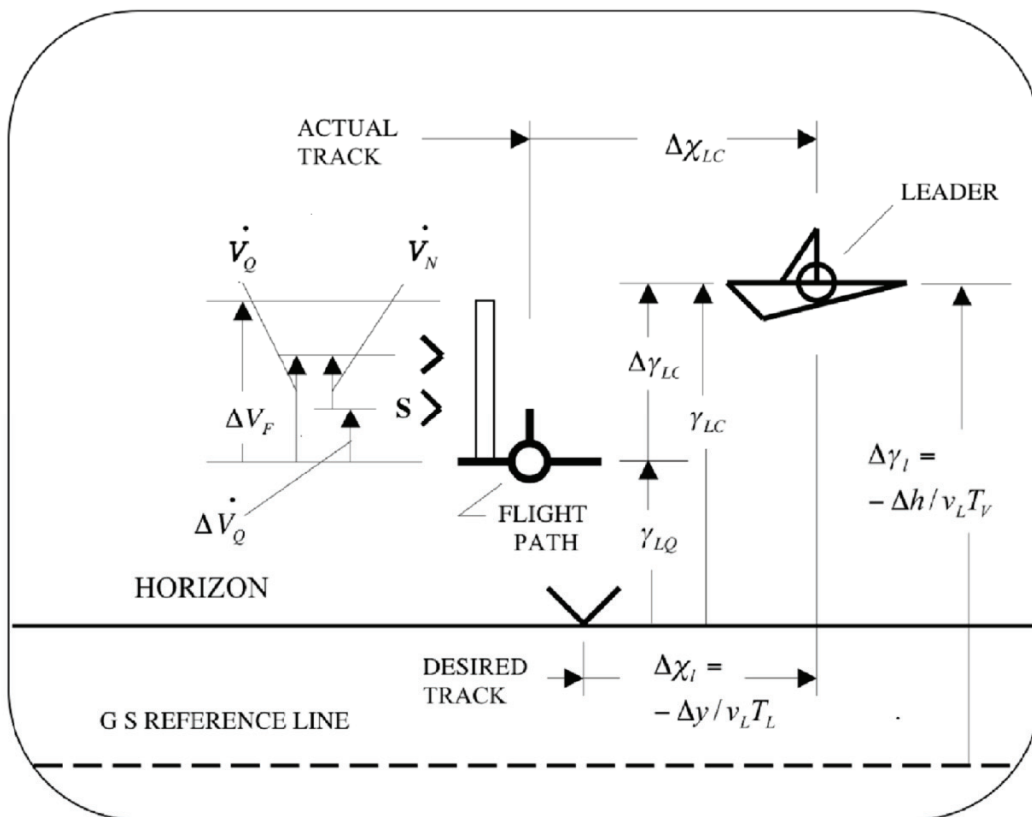


Figure 4.1a. Pursuit display elements.

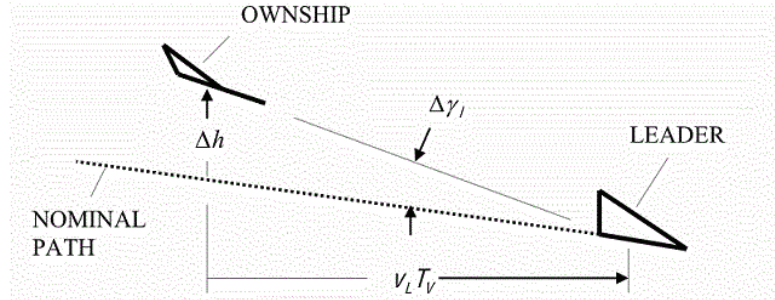


Figure 4.1b. Vertical pursuit display elements.

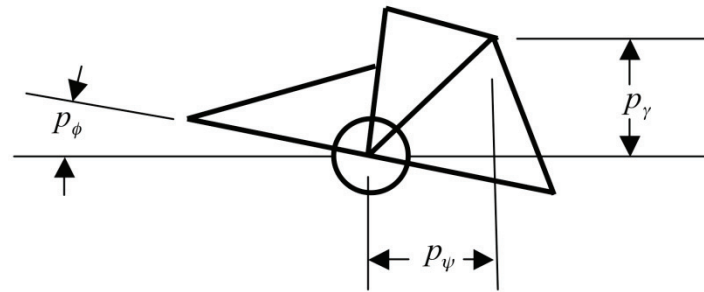


Figure 4.1c. Leader perspective angles.

Figure 4.1c shows the perspective attitudes of the leader symbol.

Figure 4.2 shows the overall configuration of the vertical flightpath, velocity, and pitch flight director displays. The following sections give the algorithms, and appendix C gives some derivations. The following symbols are used in figure 4.2:

$\Delta\chi_l$	leader's lateral track measured from the desired track,	deg
$\Delta\chi_{LC}$	limited commanded change in track,	deg
γ_L	limited vertical flightpath,	deg
γ_{LQ}	limited quickened vertical flightpath,	deg
γ_{LC}	limited commanded vertical flightpath	deg
$\Delta\gamma_l$	leader's vertical flightpath measured from the nominal path,	deg
$\Delta\gamma_{LC}$	limited commanded change in vertical flightpath,	deg
"V"	true airspeed/ground speed input to the acceleration caret,	knots
ΔV_F	displayed, gained, and filtered velocity error,	deg
ΔV_C	commanded change in velocity,	knots
v_L	limited ground speed,	fps
$\Delta \dot{V}_Q$	quickened rate of change of velocity w.r.t. the nominal (or "scheduled") value,	knots
\dot{V}_N	nominal rate of change of the true air/ground speed,	deg

\dot{V}_Q	total rate of change of the velocity,	deg
T_L	leader's lateral time constant,	sec
T_V	leader's vertical time constant,	sec
K_S	velocity scaling (≈ 3.3),	kt/deg
τ_T	turbulence smoothing filter time constant,	sec
$\Delta\theta$	difference between the actual and nominal pitch angles, $\theta - \theta_N$, (section 4.5),	deg
$\Delta\delta_T$	difference between the actual and nominal thrust lever angles, $\delta_T - \delta_{TN}$, (section 4.5),	pct
θ_C	flight director pitch command,	deg
δ_{TC}	flight director thrust lever angle command,	deg
p_ψ	lateral perspective on the leader, $b(\Delta y)/(v_L T_L)$,	deg
p_γ	vertical perspective on the leader, $b(\Delta h)/(v_L T_V)$,	deg
p_ϕ	leader's roll angle, $\tan^{-1}[\text{curv}(v_L^2)/g]$,	deg
b	leader wingspan on the HUD or PFD,	deg
Δy	lateral error from the LNAV path (positive right),	ft
Δh	vertical error from the VNAV path (positive up),	ft
curv	LNAV path curvature (1/radius),	1/ft

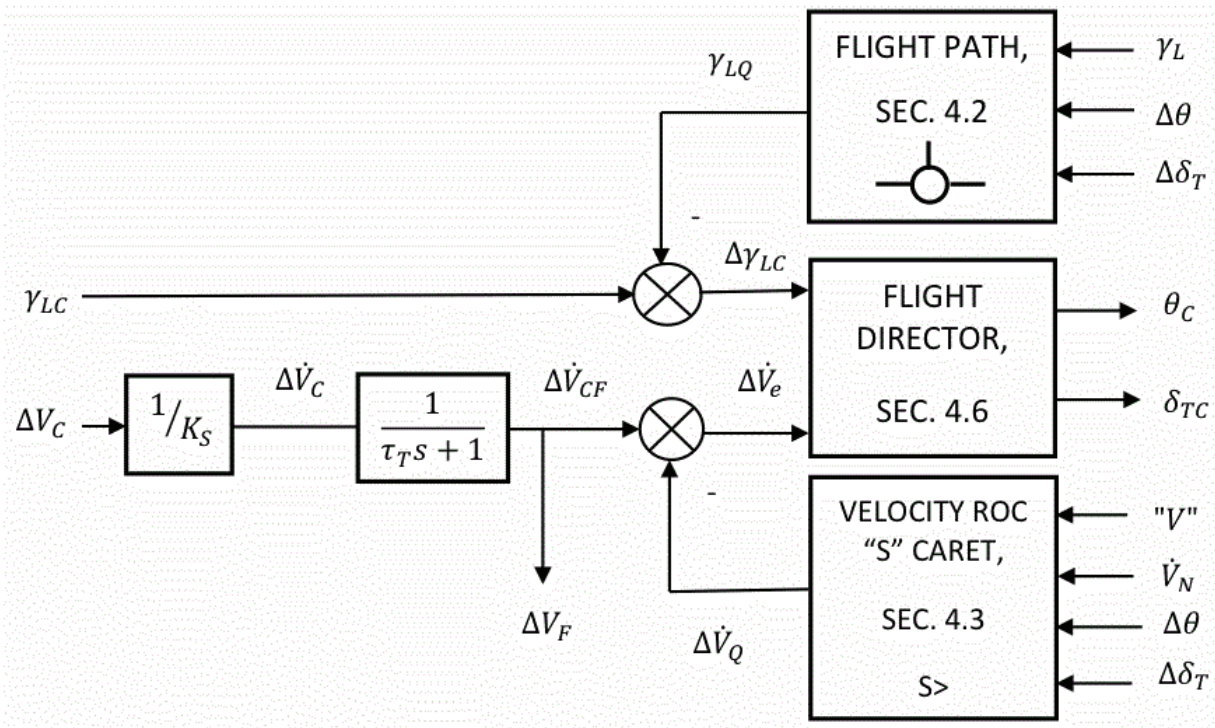


Figure 4.2. Pursuit display and pitch flight director configuration.

The flight director commands are not shown in figure 4.1. The pitch command, θ_C , is presented as a caret on the right wing tip of the flightpath symbol. The thrust lever command, δ_{TC} , is a “handle” notched into the left wing of the flightpath symbol. Figure 1.1 in section 1.0 shows the PFD with these symbols.

The “s” caret symbol in figure 4.1a is removed when $|\dot{V}_N| \leq 0.2$ degrees, indicating that the scheduled or nominal rate of change of speed is small.

The turbulence filter time constant in figure 4.2 is $\tau_T \approx 0.1$ seconds when using ground speed and $\tau_T \approx 1.5$ when using airspeed.

In figure 4.2, ΔV_C , the commanded change in velocity, is a blend between airspeed and ground speed as shown in figure 4.3.

where:

V_a	true airspeed,	knots
V_{ac}	true airspeed command,	knots
V_G	ground speed,	knots
V_{GX}	component of ground speed along the flightpath,	knots
V_{GC}	commanded ground speed,	knots
x	distance along the VNAV path, zero at the start,	ft
χ	track angle,	deg
ψ_t	nominal track angle on the LNAV path,	deg

The airspeed-to-ground speed (A/S-to-G/S) blend is calculated in the “Quickened Vel Rate-Airspd/Grndspd Blend” subsystem in the “Quickened FP & Vel Rate” subsystem in the section 5.0 Simulink model. In CTR-10 it was linear, and it occurred over the last 1500 feet of distance before touchdown if an approach to hover was being flown.

At low speeds the ground speed is limited (to v_L) in calculating display variables to preclude large (or infinite) display angles. For CTR-10 the speed was limited to 57.3 feet per second (fps) or 33.9 knots. Above this speed the display showed true angles and below this speed each degree of display was equal to 1 fps of lateral or vertical velocity.

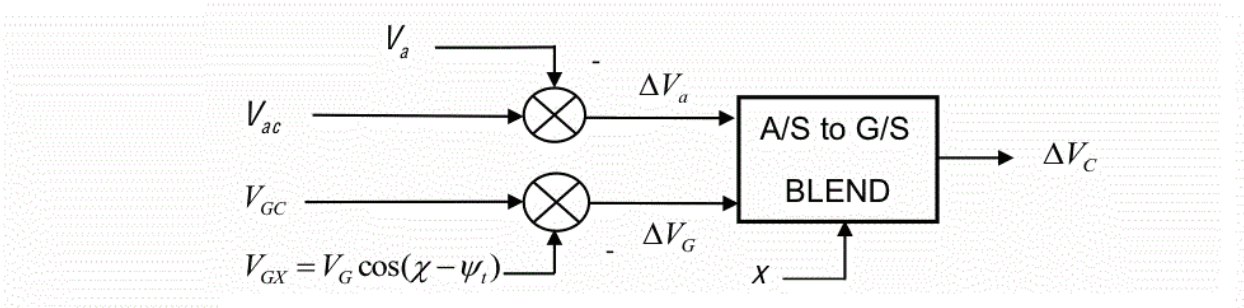


Figure 4.3. Blend of airspeed to ground speed.

4.2 Vertical Flightpath Symbol, γ_{LQ}

Figure 4.4 shows the closed-loop task for quickened flightpath angle. It shows how γ_{LQ} is generated for the display in figure 4.1a and for the input to the flight director in figure 4.2. where:

τ_H	heave time constant of the approximate first-order vehicle model,	sec
τ_e	time constant of the first-order engine model (section 4.4),	sec
γ_θ	the steady-state γ response (in the ≈ 1 - to 4-second time frame) of the vehicle to a step change in θ (δ_T fixed),	deg/deg
γ_T	the steady-state γ response (in the ≈ 1 - to 4-second time frame) of the vehicle to a step change in δ_T (θ fixed),	deg/pct

and:

$$\gamma_L = \left(\frac{180}{\pi}\right) \tan^{-1} \left(\frac{\dot{h}}{v_L}\right), \quad \text{deg}$$

The two feedback loops with dynamics in figure 4.4 provide quickening for the flightpath symbol. They eliminate the vehicle heave and engine time delays in the display and allow the pilot to close a much tighter control loop. Details of the quickening, etc. are discussed in reference 1.

The variables τ_H , τ_e , γ_θ , γ_T are stored in tables as a function of the present configuration of the vehicle, equivalent airspeed, altitude, and flightpath angle. θ_N and δ_{TN} are stored in tables as a function of the nominal configuration of the vehicle, equivalent airspeed, altitude, and flightpath angle along the VNAV path.

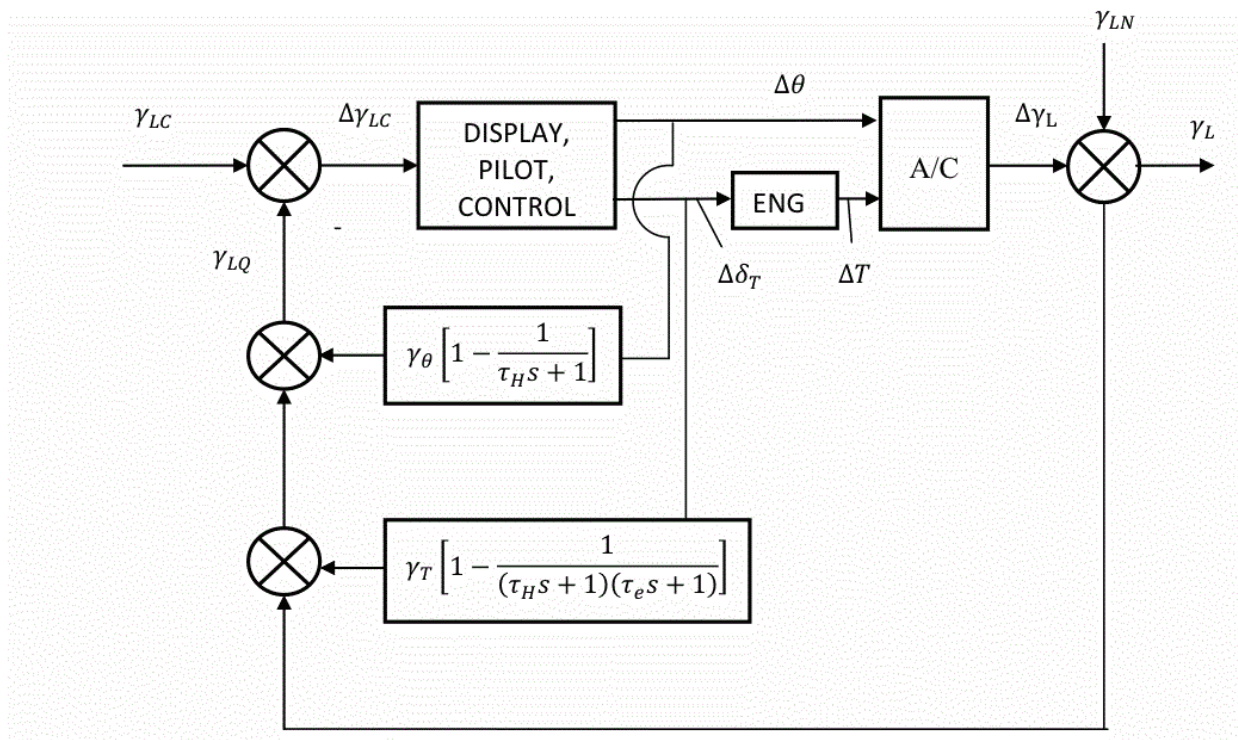


Figure 4.4. Flightpath control.

4.3 Velocity Rate of Change Caret, $\Delta\dot{V}_Q$

Figure 4.5 shows the closed-loop task for the control of velocity rate. It shows how $\Delta\dot{V}_Q$ is generated for the display in figure 4.1a and for the input to the flight director in figure 4.2 where:

ω_F	speed filter natural frequency,	rps
ζ_F	speed filter damping ratio (≈ 0.8)	
$\Delta\dot{V}_e$	velocity rate error,	deg
\dot{V}_F	filtered rate of change of speed,	deg
$\Delta\dot{V}_F$	filtered minus nominal rate of change of speed,	deg
$\Delta\dot{V}_{CF}$	filtered commanded rate of change of speed (fig.4.2),	deg
\dot{V}_θ	steady-state rate of change of airspeed (in the ≈ 1 - to 4 - second time frame) of the vehicle to a step change in θ (δ_T fixed),	deg/deg
\dot{V}_T	steady-state rate of change of airspeed (in the ≈ 1 - to 4 - second time frame) of the vehicle to a step change in δ_T (θ fixed),	deg/pct

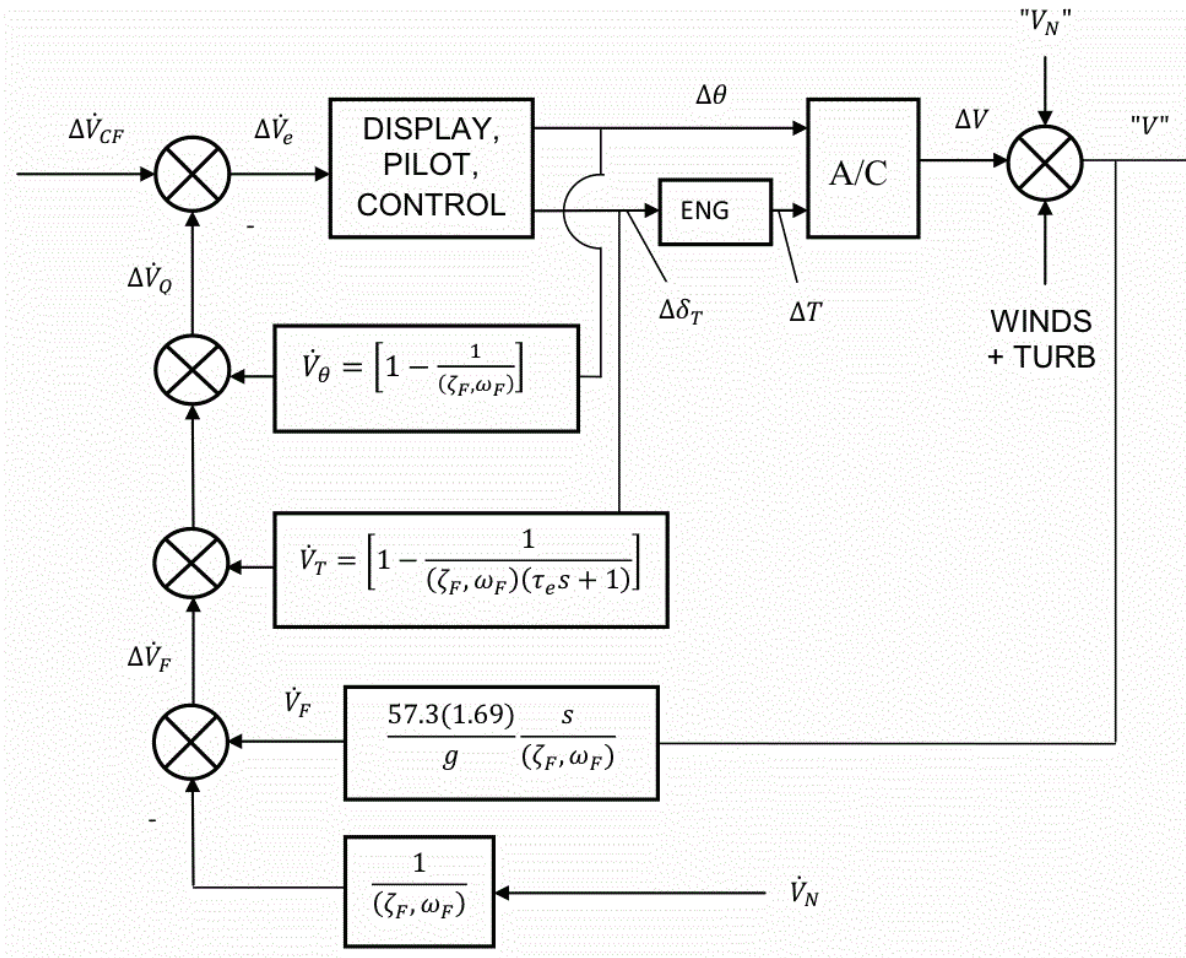


Figure 4.5. Velocity rate control.

where:

$$(\zeta_F, \omega_F) = (s/\omega_F)^2 + \left(2\zeta_F/\omega_F\right)s + 1.$$

The upper two feedback loops in figure 4.5 provide quickening for the velocity-rate symbol, $\Delta\dot{V}_Q$. They compensate for the filtering on "V" and \dot{V}_N and allow the pilot to close a much tighter control loop. Details of the quickening, etc. are discussed in reference 1.

The variables \dot{V}_θ and \dot{V}_T are stored in tables as a function of the present configuration of the vehicle, equivalent airspeed, altitude, and flightpath angle.

The speed filter natural frequency used in CTR-10 was $\omega_F \approx 2.0$ when using ground speed and 0.3 when using airspeed.

The variable ω_F and the speed input "V" varied linearly between the airspeed and ground values as is done for the A/S-to-G/S speed blend in figure 4.3.

The nominal rate of change of true airspeed/ground speed, \dot{V}_N , can use Eq. (4.6) in section 4.5 for airspeed rate and \dot{v}_G from VNAV for ground-speed rate after converting the dimensions to degrees. They vary between them linearly the same as for the speed input, "V".

If wind information is not available or the wind is constant, then from Eq. (4.4) in section 4.5, $\dot{v}_A \approx \dot{v}_G$ from VNAV. This was used in CTR-10 and RASCAL and is what the Simulink model in section 5.0 uses.

4.4 Engine Model

For a vehicle with collective control for thrust, the time constant τ_e in the linearized engine model in figures 4.4 and 4.5 is approximately zero. For a conventional engine, such as on a conventional takeoff and landing (CTOL) vehicle, the time constant can be on the order of seconds. In addition, on a conventional engine there is usually a significant nonlinearity between the thrust lever position, δ_T , and thrust. Since the response of the vehicle in γ or \dot{V} is almost proportional to thrust, the sensitivities (γ_T and \dot{V}_T in figs. 4.4 and 4.5) should be to an intermediate variable with the non-linearity approximately removed. For a "B757/A320" CTOL class vehicle simulation, ΔT was used, where:

$$\Delta T = T - T_N, \text{ percent} \quad (4.1)$$

$$T = T_0 + T_1\delta_T + T_2\delta_T^2, \text{ percent} \quad (4.2)$$

$$\text{with: } T_0 = 0, T_1 = 0.12, T_2 = 0.0088$$

The variable T_N was the thrust from the γ/V diagrams for this model. ΔT was used for the quickening feedbacks in figures 4.4 and 4.5 in place of $\Delta\delta_T$ for this vehicle.

The model in section 5.0 assumes that steady-state thrust is proportional to throttle position.

4.5 Nominal Pitch, θ_N , and Thrust Lever Angle, δ_{TN} (or T_N)

To determine θ_N and δ_{TN} (or T_N from section 4.4) for use in figures 4.2, 4.4, and 4.5, use the γ/V diagrams discussed in section 3.1.3. Enter these diagrams with vehicle nominal configuration, altitude, and equivalent airspeed, and for flightpath angle use:

$$\gamma_{\gamma V} = \gamma \frac{v_G}{v_A} + \frac{180}{\pi} \frac{\dot{v}_{GA}}{g}, \quad \text{deg} \quad (4.3)$$

with:

$$\dot{v}_{GA} = \dot{v}_A + \dot{v}_W \cos(\psi - \psi_W) + v_W \sin(\psi - \psi_W) \dot{\psi}_W, \quad \text{fps}^2 \quad (4.4)$$

$$\psi = \psi_t + \sin^{-1} \left[\frac{v_W}{v_A} \sin(\psi_t - \psi_W) \right], \quad \text{deg} \quad (4.5)$$

$$\dot{v}_A \approx \sigma^{-0.5} \left[\dot{v}_e + \frac{v_e v_G}{2H} \tan \gamma \right], \quad H \approx 26,000, \quad \text{fps}^2 \quad (4.6)$$

$$\dot{v}_W = \frac{dv_W}{dh} v_G \tan \gamma, \quad \text{fps}^2 \quad (4.7)$$

$$\dot{\psi}_W = \frac{d\psi_W}{dh} v_G \tan \gamma, \quad \text{rps} \quad (4.8)$$

where:

γ	inertial flightpath angle,	deg
v_G	ground speed,	fps
v_A	true airspeed,	fps
\dot{v}_{GA}	component of rate of change of ground speed along the true airspeed,	fps ²
v_e	equivalent airspeed,	fps
\dot{v}_e	rate of change of equivalent airspeed from VNAV,	fps ²
v_W	magnitude of the horizontal component of the wind vector,	fps
ψ	nominal vehicle heading in the presence of wind,	rad
ψ_W	heading of the wind vector (positive with the wind),	rad
σ	the atmospheric density ratio	

The variables dv_W/dh and $d\psi_W/dh$ come from the wind profile as a function of altitude.

With these coordinates for V and γ , obtain values for $\theta_{\gamma V}$ and $\delta_{\gamma V}$ (or $T_{\gamma V}$) from the γ/V diagrams. $\theta_{\gamma V}$ must be corrected for \dot{v}_{GA} to get θ_N . For the “B757/A320” simulation, $T_{\gamma V}$ was also corrected for altitude as the γ/V diagrams were for 2500 feet.

$$\theta_N = \theta_{\gamma V} - 57.3 \frac{\dot{v}_{GA}}{g}, \quad \text{deg} \quad (4.9)$$

$$T_N = \frac{P_{2500}}{P} T_{\gamma V}, \quad \text{pct} \quad (4.10)$$

where:

P	atmospheric pressure
P_{2500}	atmospheric pressure at 2500 feet

The inputs to Eqs. (4.3) through (4.10) come from VNAV and LNAV. If VNAV (and LNAV) are not engaged, then θ_N and δ_{TN} (or T_N) are set to zero. If the wind is small or constant, from eq. (4.4), $\dot{v}_{GA} = \dot{v}_A$.

Since the nominal values of pitch and thrust lever angle are washed out (see Figs. 4.4 and 4.5), the rate of change of these parameters is more important than the absolute value.

4.6 Flight Director

There are several modes for the flight-director commands (θ_C and δ_{TC} in fig.4.2) used for different flight conditions.

4.6.1 Flight Condition (1): Fixed Throttle Speed on Elevator

$$\theta_C = -\Delta\dot{V}_e, \text{ deg} \quad (4.11)$$

$$\delta_{TC} = \delta_T - \delta_{TFC}, \text{ pct} \quad (4.12)$$

where:

δ_{TFC} is the fixed throttle lever command.

4.6.2 Flight Condition (2): Fixed Throttle Path on Elevator

$$\theta_C = \Delta\gamma_{LC}, \text{ deg} \quad (4.13)$$

$$\delta_{TC} = \delta_T - \delta_{TFC}, \text{ pct} \quad (4.14)$$

4.6.3 Flight Condition (3): Closed Loop on Speed and Path

$$\begin{pmatrix} \theta_C \\ \delta_{TC} \end{pmatrix} = \begin{pmatrix} \theta_\gamma & \theta_{\dot{V}} \\ \delta_\gamma & \delta_{\dot{V}} \end{pmatrix} \begin{pmatrix} \Delta\gamma_{LC} \\ \Delta\dot{V}_e \end{pmatrix}, \quad \begin{pmatrix} deg \\ pct \end{pmatrix} \quad (4.15)$$

where:

$$\begin{pmatrix} \theta_\gamma & \theta_{\dot{V}} \\ \delta_\gamma & \delta_{\dot{V}} \end{pmatrix} = \begin{pmatrix} \gamma_\theta & \gamma_T \\ \dot{V}_\theta & \dot{V}_T \end{pmatrix}^{-1} = \frac{1}{\gamma_\theta \dot{V}_T - \gamma_T \dot{V}_\theta} \begin{pmatrix} \dot{V}_T & -\gamma_T \\ -\dot{V}_\theta & \gamma_\theta \end{pmatrix} \quad (4.16)$$

where γ_θ and γ_T are defined for vertical flightpath control (fig. 4.4) and \dot{V}_θ and \dot{V}_T are defined for velocity control (fig. 4.5). If an intermediate variable, such as T (Eqs. 4.1 and 4.2), is being used instead of δ_T , then γ_T and \dot{V}_T in Eq. (4.16) are with respect to T instead of δ_T . Then the thrust command in Eq. (4.15) will be T_C instead of δ_{TC} and Eq. (4.2) must be solved for the pilot's inceptor command, δ_{TC} , from T_C .

$$\delta_{TC} = \frac{-T_1 \pm \sqrt{T_1^2 - 4T_2(T_0 - T_C)}}{2T_2}, \quad \text{pct} \quad (4.17)$$

4.6.4 Flight Condition (4): TOGA, Fixed Throttle and Fixed θ

$$\theta_C = \theta - \theta_{GA}, \text{ deg} \quad (4.18)$$

$$\delta_{TC} = \delta - \delta_{TGA}, \text{ pct} \quad (4.19)$$

Eqs. (4.18) and (4.19) are used initially in the TOGA mode until reaching the TOGA equivalent airspeed, V_{eGA} , when the mode switches to flight condition (1) with $V_{ac} = \sigma^{-0.5}V_{eGA}$ in figure 4.3. A delta on the desired speed, V_{eGA} , is used for switching modes to prevent overshooting. When nearing the desired TOGA altitude, the mode switches to flight condition (3) when $\Delta\gamma_{LC} = 0$ in figure 4.4.

In these flight conditions, a positive θ_C is a pitch-up command and the flight-director caret is above the wing tip of the flightpath symbol. A positive δ_{TC} is an increase-power command and the flight-director “handle” is below the left wing of the flightpath symbol.

4.7 Mode Control and RNAV Capture

For full functionality, the flight director needs a pilot interface for mode selection. For the PPGD system in the U.S. Army RASCAL Black Hawk, the flight director was interfaced through an onboard PC.

For the present PPGD code the system initially defaults to flight condition (3) (section 4.6) and uses a simple set of logic for LNAV and VNAV capture. The LNAV capture logic is:

If: $|\Delta y| \leq 1000$ ft

then LNAV captures. Once LNAV is captured, the VNAV capture logic is armed and is:

If: $|\Delta h| \leq 500$ ft

then VNAV captures. The LNAV and VNAV capture thresholds are externally set constants (fig. 5.2).

When TOGA is engaged, the system goes, in sequence, to flight conditions (4) and (1) as discussed in section 4.6.4. No level-out at TOGA altitude is provided for in the present PPGD model in section 5.0.

5.0 PPGD SIMULINK MODEL

A conceptual layout of the Simulink model showing the inputs, outputs, and major subsystems is shown in figure 5.1. The inputs on the left from the aircraft (or simulator) and the outputs on the right from the model to the displays are described in section 6.0. The data required inside the model are described in section 7.0. Figure 5.2 is a MATLAB m file for constants that can be inputs such as those for describing the LNAV path.

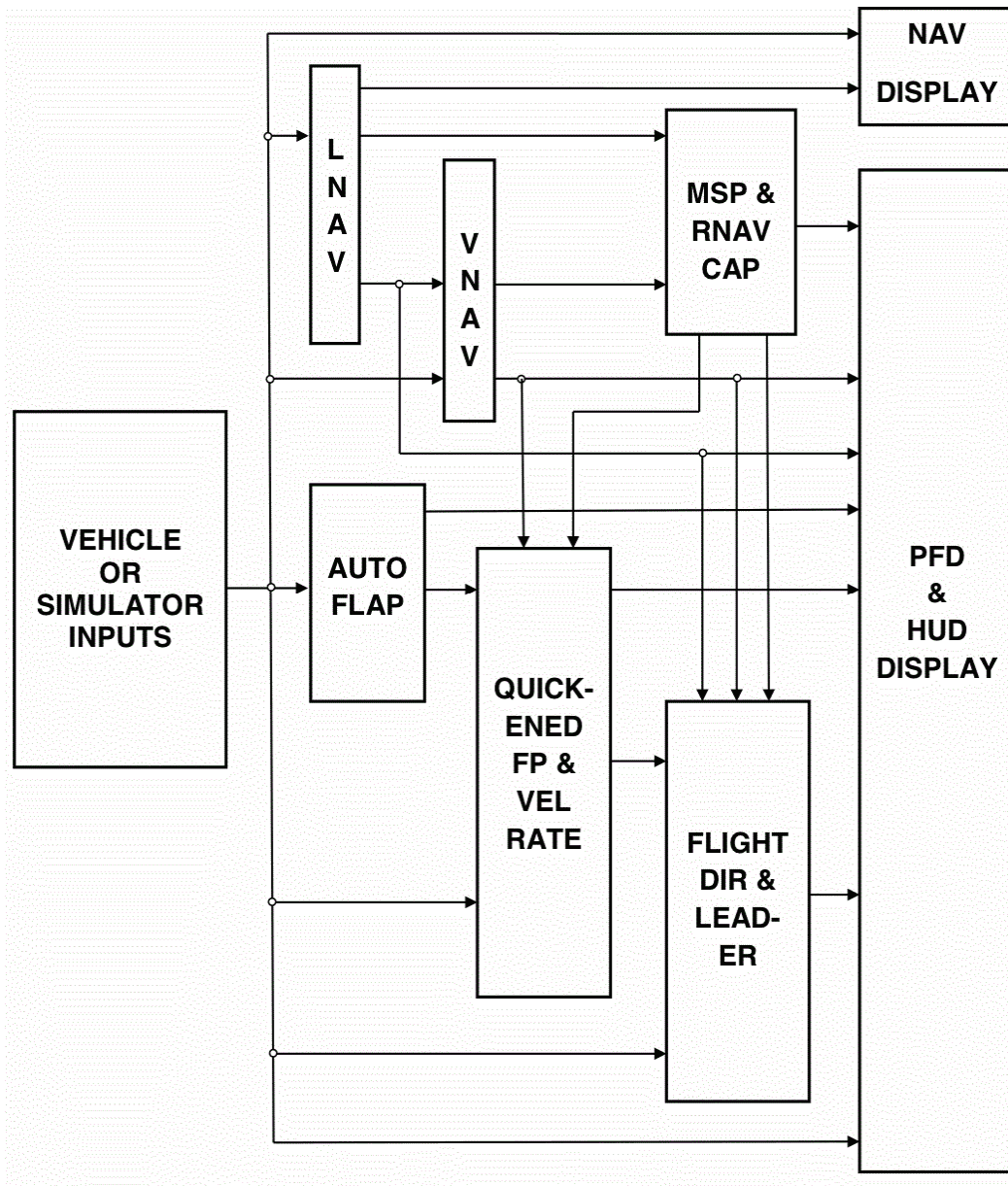


Figure 5.1. PPGD conceptual Simulink model.

```

% PPGD_111031_input_constants.m
%
% LNAV path inputs in runway coordinates (SFO 28R)
lat_rw_deg=37.613529205322;
lon_rw_deg=-122.3571395874;
psi_rw_deg=296.238;
df_ft=4757;
dir_n=1;
rn_ft=3000;
x_nm1_ft=35000;
y_nm1_ft=6000;
rnm1_ft=10000;
x_nm2_ft=35000;
y_nm2_ft=19000;
initial_seg=1;
k_bank_lead=0.5;
lead_phidot=3;
%
% convert runway coordinate LNAV inputs to latitude and longitude
lat_rw_rad=lat_rw_deg*(pi/180);
psi_rw_rad=psi_rw_deg*(pi/180);
lat_np1_deg=lat_rw_deg;
lon_np1_deg=lon_rw_deg;
lat_nm1_deg=lat_rw_deg+(60*6076.1)^(-1)*(x_nm1_ft*cos(psi_rw_rad)-
y_nm1_ft*sin(psi_rw_rad));
lon_nm1_deg=lon_rw_deg+(60*6076.1)^(-
1)*(x_nm1_ft*sin(psi_rw_rad)+y_nm1_ft*cos(psi_rw_rad))/cos(lat_rw_rad);
lat_nm2_deg=lat_rw_deg+(60*6076.1)^(-1)*(x_nm2_ft*cos(psi_rw_rad)-
y_nm2_ft*sin(psi_rw_rad));
lon_nm2_deg=lon_rw_deg+(60*6076.1)^(-
1)*(x_nm2_ft*sin(psi_rw_rad)+y_nm2_ft*cos(psi_rw_rad))/cos(lat_rw_rad);
%
% other PPGD input constants
ext_fp_on_01=0;
hrw=13;
cg_gear=20;
Vega=120;
lnav_cap_thress=1000;
vnav_cap_thress=500;
flare_gain=-0.15;
hdotd_bias=-5.6;
toga_alt_bug_ft=2000;
weight_gross_lbf=195000;
not_imode=99;
Vg_min=1.0;

```

Figure 5.2. PPGD input constants MATLAB m file.

6.0 PPGD INTERFACES TO THE AIRCRAFT (OR SIMULATOR) AND TO THE DISPLAY

6.1 General

The LNAV, VNAV, flightpath pursuit display, velocity control, and flight-director algorithms of sections 2.0, 3.0, and 4.0 are programmed into the figure 5.1 MathWorks Simulink model. The interfaces between PPGD and the aircraft (or simulator) and the displays are discussed in the following three subsections.

6.2 Aircraft (or Simulator) Interface

Each input variable from the aircraft or simulator required for the PPGD model is discussed in order:

roll	aircraft roll attitude,	deg
heading	conventional aircraft Euler angle true heading,	deg
h _{dot}	rate of climb,	fps
alt _{set}	altimeter setting,	in Hg
y _{ddot}	lateral acceleration at the center of gravity (c.g.),	fps ²
lat _{veh_deg}	vehicle latitude,	deg
lon _{veh_deg}	vehicle longitude,	deg
imode	triggers LNAV path generation during a simulation run,	
gen _{new_path}	generates a new LNAV path in simulator initial condition,	
h	altitude above mean sea level (MSL),	feet
trk	true track angle,	deg
mcp _{toga_mode}	engages the TOGA mode; 0 is no TOGA; 1 is TOGA engaged	
manual _{flap}	flap angle (or other configuration variable, e.g., nacelle, from an external selector if auto _{flaps} is not used),	deg
V _e	equivalent airspeed,	knots
V _g	ground speed,	knots
thet	pitch attitude,	deg
throt	throttle position,	pct
gear _{dn}	gear up/down; 0 is gear up, 1 is gear down	
ext _{fp}	vertical flightpath angle from an external source,	deg
ext _{fp_on_01}	input constant that enables the external flightpath, 0 off, 1 on	
weight _{gross_lbf}	vehicle gross weight,	lbs
hrw	input constant for the runway MSL altitude at the glide-slope intercept point,	feet
cg _{gear}	input constant for the height of the center of gravity of the vehicle above the main landing gear,	feet

6.3 NAV Display Interface

If it is desired to draw the LNAV path on a NAV display, the “NAV Inav path” bus in the Simulink model provides the latitude and longitude of the start and end of the turn arcs, the latitude and longitude of the arc centers, the heading for arc starts, the arc lengths in degrees and feet (dn,dnm1), and the latitude and longitude of the start and end of the great-circle segments.

The “NAV DOTS” MATLAB function provides outputs for five predictor dots for the NAV display. The x and y coordinates are in aircraft body axes. In the model in figure 5.1 the dots are spaced 2 seconds apart for a total of 10 seconds of prediction.

6.4 PFD and HUD Display Interface

A typical PFD format with pursuit guidance is shown in figure 1.1. A typical HUD format is similar. Each output variable from the PPGD model to the PFD or HUD display is discussed in order. The flightpath, fp, and leader display coordinates, X and Y, are measured from the center of the display. X is positive to the right and Y is positive up.

pitch_deg	aircraft pitch attitude,	deg
roll_deg	aircraft roll attitude,	deg
heading_deg	aircraft true heading attitude,	deg
throttle_%	throttle position (the tape to the right of the airspeed tape),	pct
GS_ref_deg	nominal VNAV glide-slope angle (dashed line parallel to the horizon),	deg
nom_track_deg	nominal LNAV true track angle (symbol above the horizon line),	deg
radar_alt_ft	radar altitude (digital readout lower center of the main display),	feet
airspeed_tape_kt	calibrated airspeed (airspeed tape drive),	knots
airspeed_bug_kt	reference speed (airspeed tape bug and digital value above the tape),	knots
grnd_speed_kt	ground speed (digital value below the airspeed tape),	knots
altitude_tape_ft	altitude above MSL (altitude), tape drive),	feet
altitude_bug_ft	reference altitude (altitude tape bug and digital value above the tape),	feet
climb_rate_fpm	rate of climb (tape to the right of the altitude tape),	fpm
alt_set	altimeter setting (digital value below altitude tape),	in Hg
app_fd_ann_01	approach mode annunciation off/on switch - display APP in all three annunciators	
side_slip_ball	side-slip ball displacement (bottom center of the display in the PFD HSI),	balls
PFD_s_caret_deg	s caret position w.r.t. the left wing of the flightpath symbol (positive up),	deg

PFD_carets_caret_deg	caret position w.r.t. the s_caret (positive up),	deg
HUD_V_error_tape_deg	velocity error-tape position (left wing of the flightpath symbol - up for fast),	deg
PFD_fd_throt_cmd_deg	throttle flight director command (handle on left wing-down for increase throttle command),	deg
PFD_leader_gamma_deg	flightpath angle of the leader symbol,	deg
PFD_leader_trk_deg	true track of the leader symbol,	deg
leader_bank_deg	roll angle of the leader symbol,	deg
HUD_leader_vert_perspect_deg	leader vertical perspective angle (positive nose up),	deg
HUD_leader_lateral_perspect_deg	leader lateral perspective angle (positive nose right),	deg
vert_error_dots	VNAV deviation (scale on right of displays),	dots
dist_to_go_nm	LNAV distance to go on the NAV display (digital upper right of display),	nm
air2ground_Vel_blend_01	annunciates VNAV speed reference - air or ground speed (AIR/GRND blend in upper right of display); presently not used	Boolean
lat_error_dots	LNAV deviation (scale on bottom of displays),	dots
flap_deg	flap angle,	deg
TOGA_fd_ann_01	TOGA mode annunciation on switch - display TOGA in all three annunciators	Boolean
flare_cue_gamma_deg	gamma position of the HUD flare cue (not shown in fig. 1.1),	deg
fd_on_01	flag to turn on the flight-director command symbols,	Boolean
fp_thick_01	flag to make the flightpath symbol thick,	Boolean
pitch_ref_thick_01	flag to make the pitch reference symbol thick,	Boolean
GS_ref_thick_01	flag to make the glide-slope reference symbol thick,	Boolean
GS_ref_on_01	flag to turn the glide-slope reference symbol on,	Boolean
vert_dots_on_01	flag to turn the VNAV deviation scale on,	Boolean
flare_cue_on_01	flag to turn the flare cue symbol on,	Boolean
radar_alt_on_01	flag to turn the radar altitude digital symbol on,	Boolean
PFD_s_caret_on_01	flag to turn the s caret symbol on,	Boolean
fd_ann_on_01	flag for the flight-director annunciator, FD, on,	Boolean
leader_on_01	flag to turn the leader symbol on,	Boolean
HUD_fp_X_deg	X position of the flightpath symbol in display coordinates,	deg
HUD_leader_X_deg	X position of the leader symbol in display coordinates,	deg
HUD_fp_Y_deg	Y position of the flightpath symbol in display coordinates,	deg
HUD_leader_Y_deg	Y position of the leader symbol in display coordinates,	deg
PFD_fp_X_deg	X position of the flightpath symbol in display coordinates,	deg
PFD_leader_X_deg	X position of the leader symbol in display coordinates,	deg
PFD_fp_Y_deg	Y position of the flightpath symbol in display coordinates,	deg
PFD_leader_Y_deg	Y position of the leader symbol in display coordinates,	deg

HUD_fp_blink_on_01	flag to blink the flightpath symbol,	Boolean
PFD_fp_blink_on_01	flag to blink the flightpath symbol,	Boolean
leader_blink_slow_on_01	flag to blink the leader symbol slow on,	Boolean
PFD_leader_vert_perspect_deg	leader vertical perspective angle (positive nose up),	deg
PFD_leader_lateral_perspect_deg	leader lateral perspective angle (positive nose right),	deg
PFD_fd_pitch_cmd_deg	pitch flight-director command (caret on right wing of the flightpath symbol - up for pitch-up command),	deg
PFD_V_error_tape_deg	velocity error tape position (left wing of the flightpath symbol - up for fast),	deg
HUD_caret_deg	caret position w.r.t. the left wing of the flightpath symbol (positive up),	deg
gear_dn	flag for gear down	Boolean
HUD_approach_Mode_on_01	flag to turn on the approach mode of the HUD,	Boolean
HUD_leader_blink_on_01	flag to blink the leader symbol,	Boolean
PFD_leader_blink_on_01	flag to blink the leader symbol,	Boolean

If magnetic headings are used on the PFD or the HUD, magnetic variation needs to be applied to the “heading_deg”, “nom_track_deg”, and “PFD_leader_trk_deg” output variables. They are given with respect to true north in the output.

7.0 SIMULINK MODEL DATA REQUIREMENTS

7.1 General

Section 6.0 describes the inputs from the aircraft (or simulator) and outputs to the displays for the Simulink model. This section describes the vehicle and display-system data required inside the PPGD model. The top-level diagram in the figure 5.1 model has seven first-level subsystems, and most of them have second-level subsystems. Filters and some MATLAB Function blocks are programmed as lower-level systems. The data required at the top level are the time constants on the “yddot” and “throt” first-order low-pass input noise filters.

Most of the data required are internal to the subsystems, but several externally settable constants are given in figure 5.2. At the top-level “ext_fp_on_01” (enables external flightpath input), “weight_gross_lbf” (vehicle gross weight), “hrw” (runway altitude at glide-slope intercept), and “cg_gear” (vertical distance from the vehicle c.g. to the landing gear in the extended position) must be set.

Data for each of the subsystems and the “NAV DOTS” MATLAB Function block are discussed in the following sections.

7.2 LNAV Subsystem

The parameters for defining the LNAV path (section 2.0) are externally settable and included in figure 5.2 and described in section 2.2. Figure 5.2 is a MATLAB m function that includes a conversion of waypoints defined in runway coordinates (assuming flat Earth) into the required waypoint latitude and longitude if desired. The actual waypoint latitude and longitude should be used for longer paths.

7.2.1 Final Turn Generation Subsystem

This subsystem is an enabled MATLAB Function block that generates the required parameters for the final turn. It is enabled in the simulator initial condition mode such that it calculates only once. No internal data are required.

7.2.2 NM1 Turn Generation Subsystem

This subsystem is an enabled MATLAB Function block that generates the required parameters for the turn before the final turn (turn n minus 1). It is enabled to calculate only once as in section 7.2.1. No internal data are required. This subsystem can be duplicated for additional turns.

7.2.3 RUN MATLAB Function Block

This subsystem is a MATLAB Function block that calculates the necessary real-time outputs for guidance and control and for display. No internal data are required.

7.2.4 PERSP_BANK Subsystem

This subsystem calculates the leader bank angle for turn anticipation. It also calculates a gain, k_{trk} , to reduce the track-command gain during turn anticipation in the flight director. No internal data are required.

7.3 Auto-Flap Subsystem

This subsystem generates an auto-flap angle as a function of “ V_e ” and “ $toga_sw$ ” and drives the flap position if the “FLAP SELECTOR Manual Switch” is in the auto-flap position. The time constant on the “ V_e ” first-order low-pass noise filter must be set. The “ $toga\ flap$ ” value must be set and the velocity value in the less-than block needs to be set to match the TOGA flap value in the flap table. The nominal approach values in the “flap table”, as a function of V_e , need to be set if it is desired to have auto flaps. The flap rate must be set in the limiter on the right.

If the “FLAP SELECTOR Manual Switch” is in the manual flap position, an external signal, “ $manual_flap$ ”, drives the flap angle.

7.4 VNAV Subsystem

This subsystem generates a VNAV path as a function of distance to go to the glide-slope intercept with the runway, “ $2cir_dist$ ”. It outputs nominal flightpath, altitude, velocity rate, and velocity. The only data required at this first level is “ xrw_vnav ”, the total distance covered by the VNAV path.

7.4.1 VNAV Tables Subsystem

Data from “Table 3.1 VNAV SEGMENT ENDPOINTS” are entered into the seven one-dimensional tables in this subsystem. The temporary constant, “ $table\ bias$ ”, is a correction for an error in the present table data.

7.4.2 gam Subsystem

This subsystem generates the VNAV nominal flightpath, “ $gamnom$ ”, from the table data. No data are required.

7.4.3 h Subsystem

This subsystem generates the VNAV nominal altitude, “ $hnom$ ”, from the table data. No data are required.

7.4.4 VEL MATLAB Function Block

This MATLAB Function block generates the VNAV nominal velocity rate, “ $Vdotnom$ ”, and velocity, “ $Venom_vnav$ ”, from the table data. No data are required.

7.5 Quickened FP & Vel Rate Subsystem

This subsystem generates quickened flightpath and velocity rate. At this level, the lower limit in the “Saturation” block for the calculation of “gam1” should be set. It is presently set at 57.3 fps (33.9 knots) to make angles below this speed equal to one fps/deg of display. The time constant on the filter on “Ve” needs to be set (presently 1 second).

7.5.1 Gamma and Vdot Sensitivity Tables Subsystem

This subsystem generates the sensitivities of flightpath and velocity rate to pitch and throttle that are used in the quickening subsystems. It also generates the heave time constant. These variables are in general a function of present gear, flap (or, e.g., nacelle), altitude, flightpath angle, and equivalent velocity values. For the cruise-efficient short take-off and landing (CESTOL) vehicle data used in this subsystem, the gear position was assumed to have negligible effect on the sensitivities. The table data were taken from the steady-state response of flightpath angle and velocity rate to pitch and throttle steps in the 1- to 4-second time frame for various flap angles. The heave time constant was obtained from the flightpath time response to a step throttle input. These data were generated at 2000 feet MSL altitude and at 195,000# gross weight. Simple corrections for different altitudes and weights were then made. For other vehicles, it may be necessary or possible to generate tables with more or less dimensions. “gamma/V alt” and “gamma/V wgt” should be set to the values for the gamma/V diagrams used. The five three-dimensional tables need data as a function of limited flightpath angle (“gam1”), filtered equivalent velocity (“VeF”), and flap angle (“flap”) as independent inputs.

As seen in subsystems “Quickened Gamma” and “Quickened Vel Rate”, the quickening generated using the sensitivities and heave time constant from these tables are washed out. Therefore, changes in the table values are more important than the absolute values.

7.5.2 Pitch and Throttle Nominal Tables Subsystem

This subsystem generates the nominal values of pitch and throttle used in the quickening subsystems. These variables are in general a function of nominal gear, flap (or, e.g., nacelle), altitude, flightpath angle, and the equivalent velocity, “Venom”. “Venom” is from the VNAV (section 7.4) for approach or from the Mode Select Panel, MSP (section 7.6) for TOGA. The table data were taken from the gamma/V diagrams for the same CESTOL in section 7.5.1 for various flap angles. These gamma/V diagrams were generated for an altitude of 2000 feet. Simple corrections for different altitudes were made. A simple correction for gear was also made, assuming the change in flightpath angle for gear up/down is proportional to velocity squared. No correction was made for the gross weight of the vehicle. For other vehicles, it may be necessary or possible to generate tables with more or less dimensions.

The “gear_up_delta_gamma” proportionality constant must be set. It is obtained from gamma/V diagrams for the two gear positions. The lower limit in the “Saturation” block is presently set at 33.9 knots (57.3 fps) to make angles below this speed equal to one fps/deg of display. “gamma/V alt” in the altitude correction logic should be set to the value for the gamma/V diagrams used. Data

for the two three-dimensional tables must be entered as a function of nominal limited effective flightpath angle (“gamgV”, $\gamma_{\gamma V}$ in section 4.5), nominal equivalent velocity (“Venom”), and flap angle (“flap”) as independent inputs.

As seen in subsystems “Quickened Gamma” and “Quickened Vel Rate”, the quickening generated using the nominal pitch and throttle from these tables are washed out. Therefore, changes in the table values are more important than the absolute values.

7.5.3 Quickened Gamma Subsystem (fig. 4.4, Flightpath Control)

This subsystem generates quickened gamma, “gamlQ”, (γ_{LQ} in fig. 4.4). The only vehicle-specific data in this subsystem is the time constant in the linearized engine model in the throttle washout. For the CESTOL model, it is set to 1 second.

7.5.4 Quickened Vel Rate Subsystem (fig. 4.5, Velocity Rate Control)

This subsystem generates the quickened rate of change of airspeed, “delVadotQ”, in the top half of the Quickened Vel Rate subsystem and ground-speed rate, “delVgdotQ”, in the bottom half. When “rnav” is captured, the one-dimensional table, “Va2Vg blend”, outputs a blend, “kag”, (0-1) as a function of LNAV distance, “2cir_dist”, to determine which is used for “delVdotQ” ($\Delta\dot{V}_Q$ in fig. 4.5). For CESTOL, the table is set to zero for all “2cir_dist” for airspeed rate only.

The filter constants for CESTOL in the airspeed rate portion are $\omega_n = 0.3$ revolutions per second (rps) and $\zeta = 0.8$, and in the ground-speed rate portion $\omega_n = 2.0$ rps and $\zeta = 0.8$. These filters smooth noise in the velocity signals and may need to be adjusted for other vehicles or missions. In addition, the time constant in the linearized engine models in the throttle washouts should be set to the desired value. For CESTOL, they were set to 1 second.

7.6 MSP & RNAV CAP Subsystem

This subsystem has no lower subsystems. It controls the flight condition (section 4.6) and LNAV and VNAV capture. Flight condition (2), fixed throttle path on elevator, is not used.

The go-around speed, “Vega”, the LNAV capture threshold, “lnav_cap_thres”, and the VNAV capture threshold, “vnav_cap_thres” are externally set constants (fig. 5.2). The time constant on the equivalent airspeed, “Ve”, first-order filter must be set. For CESTOL, 1 second was used. The constant “Vega_thres” must be set as it controls when the guidance switches from a fixed throttle-constant pitch flight condition (4) to a fixed throttle speed on elevator flight condition (1) during TOGA. The throttle reference, “throtref”, constant must be set for stall protection. When the throttle is greater than “throtref”, the flight condition changes from closed loop on speed and flightpath (3) to fixed throttle speed on elevator (1). For CESTOL, throtref=60% as the model is overpowered.

7.7 Flight Director and Leader Subsystem

This subsystem generates the pitch and throttle flight-director commands, the position and attitude of the leader symbol, and the rate of change of airspeed command, “delVdotcf” ($\Delta\dot{V}_{CF}$ in fig. 4.2). At this level the constants throttle reference (“throtref”), TOGA throttle (“throtga”), and TOGA pitch (“thetga”), must be set. For CESTOL they are throtref=throtga=60% and thetga=7 deg. “throtref” should be the same value as set in section 7.6.

7.7.1 Leader Lateral Subsystem

This subsystem generates the lateral position of the leader symbol, “trkc”, ($\Delta\chi_l$ in fig. 4.1a) and the leader lateral perspective angle, “persp_lat”, (p_ψ in fig. 4.1c).

The lower limit in the “Saturation” block must be set. It is presently set at 57.3 fps (33.9 knots) to make angles below this speed equal to one fps/deg of display. The one-dimensional table, “TL table”, generates the leader symbol lead time for approach as a function of altitude above the runway, “hag”. It is presently set to 15 seconds for altitudes greater than 1500 feet above the runway and 5 seconds for altitudes less than 100 feet, and it varies linearly between. The constant “TOGA TL” is the lead time for TOGA. The gain in the “persp_lat” path, “b_HUD”, is the wing span of the leader symbol on the HUD in degrees (4 degrees was used).

7.7.2 Leader Gamma Subsystem

This subsystem generates the vertical position of the leader symbol, “gamlc”, (γ_{LC} in fig. 4.1a) and the leader vertical perspective angle, “persp_vert”, (p_γ in fig. 4.1c).

The lower limit in the “Saturation” block must be set. It is presently set at 57.3 fps (33.9 knots) to make angles below this speed equal to one fps/deg of display. The one-dimensional table, TV table, generates the lead time of the leader symbol as a function of altitude above the runway, “hag”. It is presently set to 15 seconds for altitudes greater than 1500 feet above the runway and 5 seconds for altitudes less than 100 feet, and it varies linearly between. The gain in the “persp_vert” path, “b_HUD”, is the wingspan of the leader symbol on the HUD in degrees (4 degrees was used).

7.7.3 Del Vdot Filtered Cmd Subsystem

This subsystem generates the commanded and filtered value of speed rate, “delVdotcf”, ($\Delta\dot{V}_{CF}$ in fig. 4.2). It is proportional to speed error. It uses the air/ground speed blend, kag, from section 7.5.4 to blend air and ground values. For CESTOL, airspeed error is used at all distances. The loop gain, “1/Ks”, is set for CESTOL to 0.3 for both air and ground-speed errors. The filter time constant on airspeed error for CESTOL is set to 1.5 seconds and 0.1 seconds for ground speed.

7.7.4 FLT DIR MATLAB Function Block

This MATLAB Function block generates the pitch command, “thetc” (θ_c in fig. 4.2), and the throttle command, “throtc” (δ_{TC} in fig.4.2), from the inputs, and it contains no vehicle-specific data that requires setting.

7.8 NAV DOTS MATLAB Function Block

This MATLAB Function block generates the predictor dots for the NAV display. Other than the externally settable constant, “Vg_min” (fig. 5.2), input to the function, no data are required. If it is desired to change the spacing between the predictor dots (presently 2 seconds), then code changes would be necessary.

7.9 PFD and HUD Display Subsystem

This subsystem has subsystems for the transform of the flightpath and the leader positions in Earth coordinates to display case coordinates and for limiting and blinking the symbols. It provides the interface to the PFD and HUD and is mostly signal conditioning; it is dependent on the particular displays used. The outputs are described in section 6.0.

The flare cue parameters, “flare_gain” and “hdotd_bias”, and the TOGA level-out altitude, “toga_alt_bug_ft”, are externally settable parameters (fig. 5.2).

Many of the outputs have gain values of one for possible display gaining.

The constant block for valid radar altitude information, “radar_alt_on_01”, near the top of the subsystem must be set. It is presently 2500 feet. The time constant on the “airspeed_tape_kt” output needs to be set. It is presently set to 1 second.

Many of the display variables have static limiting that must be set as desired.

The “GS_ref_deg” output requires that the “thetga” constant be set (7 for CESTOL) and should be the same as in section 7.7.

The flare cue, “flare_cue_gamma_deg”, is a simple linear h versus \dot{h} law. The altitude to display the flare cue in the output, “flare_cue_on_01”, needs to be set. It is presently set to <400 feet. The lower limit in the left saturation block must be set. It is presently set at 57.3 fps (33.9 knots) to make angles below this speed equal to one fps/deg of display. The limiting on the “flare_cue_gamma_deg” output needs to be set. The upper limit in the right saturation block is set to limit the flare cue to approximately 3 degrees negative. The lower value, -10, keeps the symbol on the display.

The time constant on “climb_rate_fpm” should be set. It is presently set to 0.7 seconds.

The “side_slip_ball” output has a gain of 0.1 g’s per one ball displacement; it is limited to +/- three balls and should be set as desired.

“PFD_fd_throt_cmd_deg” (the flight director throttle command) output has a gain of -0.25 degrees of display per percent of throttle command (CESTOL) and should be set as desired.

The flap input to “HUD_approach_mode_on_01” must be set as desired. It is presently set to the final approach value for CESTOL, 40 degrees.

The outputs "PFD_leader_vert_persp_deg" and "PFD_leader_lateral_persp_deg" are gained up from the HUD values (sections 7.7.1 and 7.7.2) to reflect the larger wingspan on the PFD. The limiting is also increased.

"vert_error_dots" and "lat_error_dots" outputs have one-dimensional tables of display sensitivity, feet per dot of display. The tables are a function of altitude above the runway. For CESTOL, vert_error_dots are each 15 feet below 100 feet and 100 feet above 667 feet, and they vary linearly between. For CESTOL, lat_error_dots are each 18 feet below 100 feet and 120 feet above 667 feet, and they vary linearly between. These tables should be set as desired.

The output to blink the leader symbol, "leader_blink_on_slow_01", has two inputs for turn anticipation and a one-dimensional table as a function of LNAV distance to go, "2cir_dist", for VNAV glide-slope anticipation. The present inputs for turn anticipation blink the leader at a slow rate 7 to 2 seconds before the turn and can be set as desired. The table for glide-slope anticipation presently blinks the leader at the slow rate 5 seconds before the start of glide-slope capture. The table must be modified for different VNAVs and the desired anticipation time.

7.9.1 HUD and PFD Earth/Case Transform Subsystems

The four "thet bias" constant blocks need to be set. They set the distance that the zero pitch (thet) reference is with respect to the center of the display, positive up. For the present displays, it is 6 degrees for the HUD and 0 for the PFD.

7.9.2 PFD Limiting Subsystem

Limiting of the PFD flightpath and leader symbols is calculated in this subsystem. Control of symbol blinking when limited is also calculated. As discussed in section 4.1, the flightpath and leader symbols are limited in display coordinates. Display coordinates are measured from the center of the display, x laterally and y vertically. The flightpath is limited (19.5 and 13.5 degrees for x and y, respectively) and the leader is then driven with respect to the flightpath but limited in x and y (20.0 and 14.0 degrees, respectively) in the present display. Blinking of the symbols has a 0.1-degree hysteresis. These values must be set as desired for the display to be used.

7.9.3 HUD Limiting Subsystem

Limiting of the HUD flightpath and leader symbols is calculated in this subsystem. Control of symbol blinking when limited is also calculated. The present HUD has two display modes controlled by the "HUD_approach_mode_on_01" logic. There is a "Normal" mode and a de-clutter "Approach" mode. The lateral travel, x, is larger for the display elements in the "Approach" mode, and the flightpath is limited to 19.5 and 7.5 degrees in display x and y, respectively. The leader is limited to 20.0 and 8.0 degrees, respectively. When in the "Normal" mode, the flightpath x is limited to 9.5 and the leader to 10.0 degrees. Symbol blinking when limited has a 0.1-degree hysteresis. These values must be set as desired for the display to be used.

APPENDIX A: LNAV ALGORITHM DERIVATIONS

In the PPGD model in section 5.0, the LNAV subsystem is made up of four subsystems with MATLAB Function block code, three of which are enabled for one-time path generation, and one for generating real-time LNAV outputs for guidance as described in section 2.0. The first path-generation subsystem is for the final turn (n) and the second for the turn prior to the final turn (nm1, n minus 1). The “LNAV ARC SUBSY” calculates turn arc parameters for NAV display. The MATLAB code is mostly coordinate transformations, and it is self-explanatory with comments.

If it is desired to add more turns than the two presently programmed, the subsystem for turn nm1 can be duplicated for additional turns. Indices would have to be incremented.

The Perspective Bank subsystem generates bank commands for turn anticipation as described in section 2.0. Based on distance to turn entry or exit (“dist_ngate”), present ground speed (“Vg”), nominal turn radius (“curv”), and the input gain “k_bank_lead” (nominally 0.5 - amount of bank change before segment change), it generates a constant roll rate to the bank angle required for the next segment as determined by “iseg”, the LNAV segment number. It also generates an output gain, “k_trk”, for use in positioning the leader symbol laterally. It is used in the “Flight Director and Leader” subsystem.

APPENDIX B: VNAV ALGORITHM DERIVATIONS

B.1 Altitude Derivations

B.1.1 Assumptions (fig. B1)

- (1) Distance, x , is the independent variable.
- (2) The profile is made up of constant flightpath angle segments, γ , and segments with constant rate of change of γ with x , γ_x .
- (3) γ is small, $\tan \gamma \approx \gamma$.

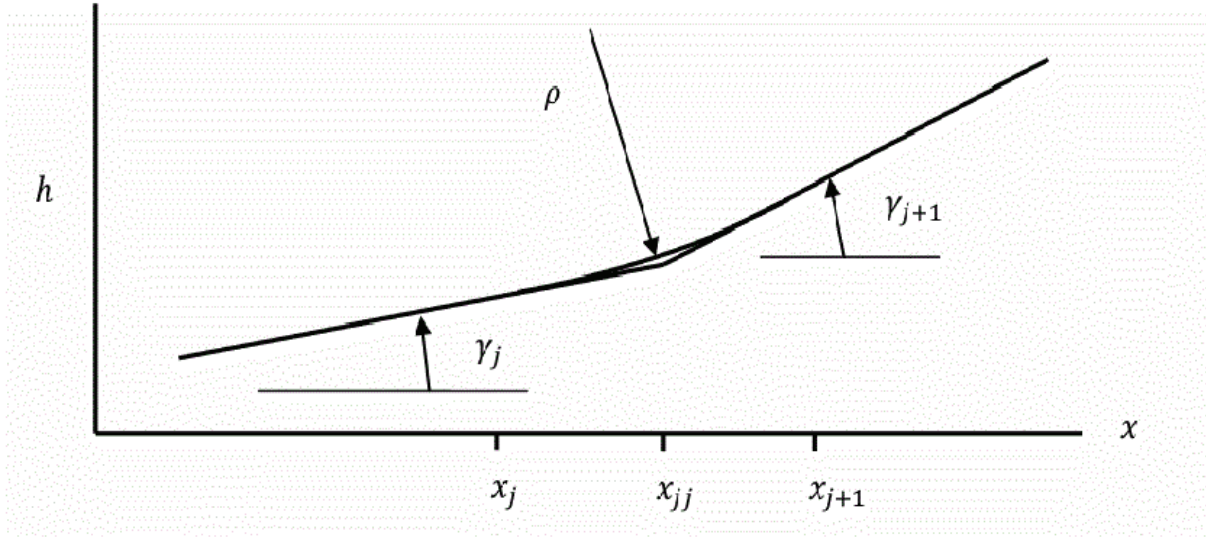


Figure B1. Altitude assumptions.

B.1.2 Flightpath Angle Transition Distance, Δx_T

$$\Delta x_T = x_{j+1} - x_j \quad (B1)$$

If ρ is the radius of curvature, assume:

$$\Delta x_T = \rho(\Delta\gamma) \quad (B2)$$

A simplified equation of motion perpendicular to the flightpath is:

$$\Delta L = \frac{W}{g} v \dot{\gamma} \quad (B3)$$

where L = lift. The change in load factor, Δn , during the γ change is:

$$\Delta n = \frac{\Delta L}{W} = \frac{v \dot{\gamma}}{g} \quad (B4)$$

Since $v = \rho\dot{\gamma}$, from Eqs. (B2) and (B4):

$$\Delta x_T = \frac{v^2(\Delta\gamma)}{g(\Delta n)} = \frac{1.69^2\pi V^2(\Delta\gamma)}{180g \Delta n} \quad (\text{B5})$$

where V is in knots and $\Delta\gamma$ is in degrees. For smooth transitions, $\Delta n \approx 0.03$ and:

$$\gamma_x = \frac{\pi \Delta\gamma}{180 \Delta x_T}, \quad \text{rad/ft} \quad (\text{B6})$$

B.1.3 Altitude Relations, h

$$d\gamma = \gamma_x dx$$

$$\gamma = \gamma_j + \gamma_x(x - x_j) \quad (\text{B7})$$

$$dh = \gamma(dx) = [\gamma_j + \gamma_x(x - x_j)]dx$$

$$\Delta h = h - h_j = \frac{\gamma + \gamma_j}{2}(\Delta x) \quad (\text{B8})$$

where $\Delta x = x - x_j$ and the total altitude change is:

$$\Delta h_T = \frac{\gamma_{j+1} + \gamma_j}{2}(\Delta x_T) \quad (\text{B9})$$

B.1.4 Distance Relations, x

From figure B1:

$$\Delta h_T = (x_{jj} - x_j)\gamma_j + (x_{j+1} - x_{jj})\gamma_{j+1}$$

From Eq. (B1) eliminate x_{j+1} and solve for x_j :

$$x_j = \frac{\Delta h_T + x_{jj}(\Delta\gamma_T) - \Delta x_T\gamma_{j+1}}{\Delta\gamma_T}$$

where $\Delta\gamma_T = \gamma_{j+1} - \gamma_j$ and from Eq. (B9), this becomes:

$$x_j = x_{jj} - \frac{\Delta x_T}{2} \quad (\text{B10})$$

and:

$$x_{j+1} = x_{jj} + \frac{\Delta x_T}{2} \quad (\text{B11})$$

Eqs. (B5), (B6), (B9), (B10), and (B11) are used to calculate the distance and altitude endpoint values in table 3.1.

B.1.5 Dynamic Values During Segments or Transitions Between Segments

Sections B.1.2 through B.1.4 give the endpoints of segments or the transitions between segments. To obtain $\gamma(x)$ and $h(x)$ for use as targets in the flight director, section 4.6, in real time use Eqs. (B7) and (B8), respectively:

$$\gamma(x) = \gamma_j + \gamma_x(\Delta x) \quad (B12)$$

$$h(x) = h_j + \frac{\gamma + \gamma_j}{2}(\Delta x) \quad (B13)$$

where:

$$\Delta x = x - x_j$$

B.2 Velocity Derivations

B.2.1 Assumptions

- (1) Distance, x , is the independent variable.
- (2) The profile is made up of constant velocity, V , segments or constant rate of change of velocity, \dot{V} , segments with short constant \ddot{V} transitions between segments.

B.2.2 Basic Relations

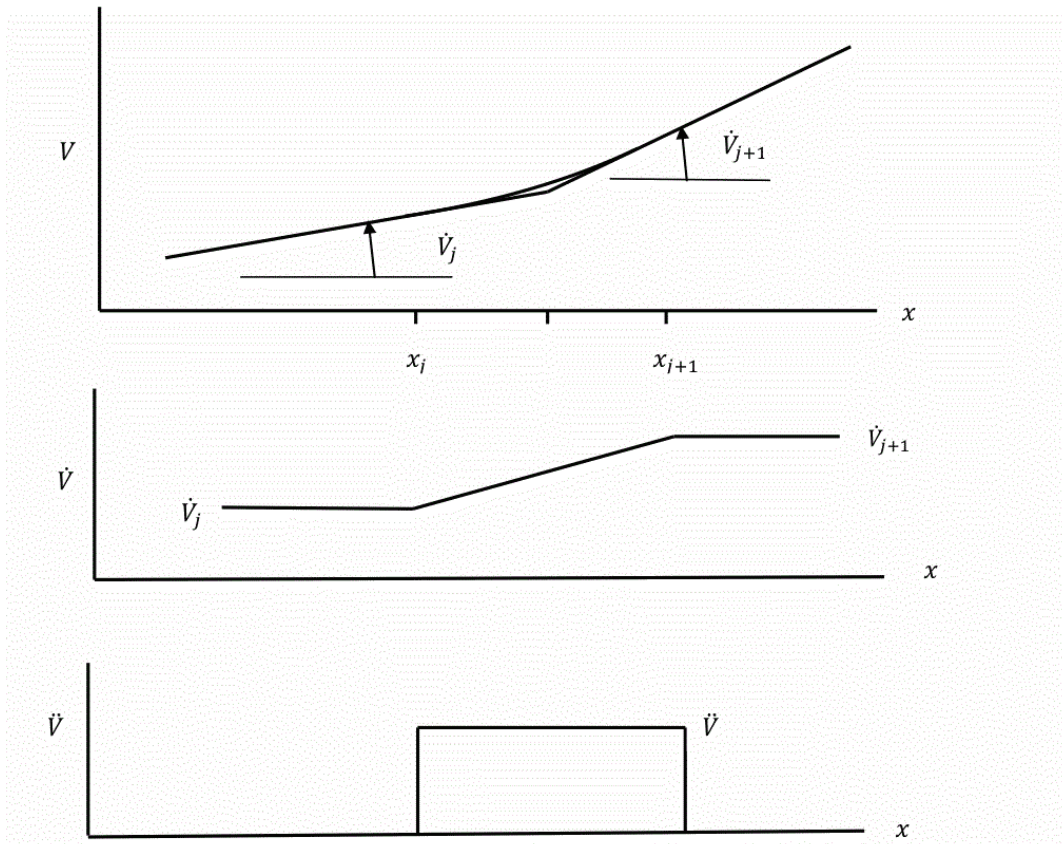


Figure B2. Velocity assumptions.

$$\Delta t = t - t_j \quad (B14)$$

$$\dot{V} = \dot{V}_j + \ddot{V}(\Delta t) \quad (B15)$$

$$V = V_j + \dot{V}_j(\Delta t) + \frac{\ddot{V}}{2}(\Delta t)^2 \quad (B16)$$

$$\frac{x}{1.69} = \frac{x_j}{1.69} + V_j(\Delta t) + \frac{\dot{V}_j}{2}(\Delta t)^2 + \frac{\ddot{V}}{6}(\Delta t)^3 \quad (B17)$$

These equations must be solved for the endpoints of the transitions between segments. Two cases are needed. The first is when the velocity change is independent of the flightpath change, and the second is when the transition between \dot{V}_j and \dot{V}_{j+1} in figure B2 is coordinated with the change in flightpath angle, γ , in figure B1.

B.2.3 Endpoints for Acceleration Change Independent of Flightpath Change

Assume:

- (1) Since \ddot{V} implies a rate of change of inceptor (throttle for a CTOL and pitch for a VTOL), assume a reasonable value ($\ddot{V} \approx 0.2$ knots/sec² would give a VTOL pitch change of about 6 degrees in 10 seconds for a 2-knot/sec change in acceleration during the transition).
- (2) \dot{V}_j and \dot{V}_{j+1} are known.

B.2.3.1 When V_j is also known, solve for ΔV_T and Δx_T :

From Eq. (B15):

$$\Delta t_T = \frac{\Delta \dot{V}_T}{\ddot{V}} \quad (B18)$$

where $\Delta \dot{V}_T = \dot{V}_{j+1} - \dot{V}_j$ and then from Eqs. (B16) and (B17):

$$\Delta V_T = \frac{\dot{V}_j(\Delta \dot{V}_T)}{\ddot{V}} + \frac{(\Delta \dot{V}_T)^2}{2\ddot{V}} \quad (B19)$$

where $\Delta V_T = V_{j+1} - V_j$ and:

$$\frac{\Delta x_T}{1.69} = \frac{V_j(\Delta \dot{V}_T)}{\ddot{V}} + \frac{\dot{V}_j(\Delta \dot{V}_T)^2}{2\ddot{V}^2} + \frac{(\Delta \dot{V}_T)^3}{6\ddot{V}^2} \quad (B20)$$

An example is the transition between segments (5) and (6) in figure 3.1 and table 3.2.

B.2.3.2 When V_{j+1} is known:

Use V_j from Eq. (B19) in Eq. (B20) to obtain:

$$\frac{\Delta x_T}{1.69} = \frac{V_{j+1}(\Delta \dot{V}_T)}{\ddot{V}} - \frac{\dot{V}_j(\Delta \dot{V}_T)^2}{2\ddot{V}^2} - \frac{(\Delta \dot{V}_T)^3}{3\ddot{V}^2} \quad (B21)$$

An example is the transition between segments (3) and (4) in figure 3.1 and table 3.2.

B.2.4 Endpoints When the Acceleration and Flightpath Change Are Coordinated

B.2.4.1 When \dot{V}_j, \dot{V}_{j+1} , and V_j are known:

Solve Eq. (B20) for \ddot{V} :

$$\frac{\Delta x_T}{1.69} \ddot{V}^2 - V_j (\Delta \dot{V}_T) \ddot{V} - (\Delta \dot{V}_T)^2 \left(\frac{\dot{V}_j}{2} + \frac{\Delta \dot{V}_T}{6} \right) = 0$$

Then:

$$\ddot{V} = \frac{-b \pm \sqrt{b^2 - 4ac}}{2a} \quad (\text{B22})$$

where:

$$\begin{aligned} a &= \frac{\Delta x_T}{1.69} \quad \text{where } \Delta x_T \text{ comes from Eq. (B5)} \\ b &= -V_j (\Delta \dot{V}_T) \\ c &= -(\Delta \dot{V}_T)^2 \left(\frac{\dot{V}_j}{2} + \frac{\Delta \dot{V}_T}{6} \right) \end{aligned}$$

Then use Eqs. (B19) and (B20) for V_{j+1} and Δx_T . Δx_T should agree with the value from Eq. (B5).

An example is the transition between segments (2) and (3) in figure 3.1 and table 3.2.

B.2.4.2 When \dot{V}_j, \dot{V}_{j+1} , and V_{j+1} are known:

Solve Eq. (B21) for \ddot{V} :

$$\frac{\Delta x_T}{1.69} \ddot{V}^2 - V_{j+1} (\Delta \dot{V}_T) \ddot{V} + (\Delta \dot{V}_T)^2 \left(\frac{\dot{V}_j}{2} + \frac{\Delta \dot{V}_T}{3} \right) = 0$$

Then:

$$\ddot{V} = \frac{-b \pm \sqrt{b^2 - 4ac}}{2a} \quad (\text{B23})$$

where:

$$\begin{aligned} a &= \frac{\Delta x_T}{1.69} \quad \text{where } \Delta x_T \text{ comes from Eq. (B5)} \\ b &= -V_{j+1} (\Delta \dot{V}_T) \\ c &= (\Delta \dot{V}_T)^2 \left(\frac{\dot{V}_j}{2} + \frac{\Delta \dot{V}_T}{3} \right) \end{aligned}$$

Then use Eqs. (B19) and (B21) for V_j and Δx_T . Δx_T should agree with the value from Eq. (B5).

Examples include the transitions between segments (1) and (2) and between segments (6) and (7) in figure 3.1 and table 3.2.

B.2.5 Endpoints for Segments with $\dot{V} = \text{Constant}$, $\ddot{V} \equiv 0$:

From Eq. (B16) with $\ddot{V} \equiv 0$:

$$\Delta t = \frac{V_{j+1} - V_j}{\dot{V}}$$

Substitute in Eq. (B17) with $\ddot{V} \equiv 0$:

$$\frac{\Delta x_T}{1.69} = \frac{V_{j+1}^2 - V_j^2}{2\dot{V}} \quad (\text{B24})$$

or:

$$\dot{V} = \frac{1.69(V_{j+1}^2 - V_j^2)}{2(\Delta x_T)} \quad (\text{B25})$$

Eq. (B25) with Eqs. (B1), (B5), and (B10) were used to obtain \dot{V} for segment (7) in figure 3.1 and table 3.2.

B.2.6 Dynamic Values During Segments or Transitions Between Segments

Sections B.2.3 through B.2.5 give the endpoints of segments or the transitions between segments in table 3.1. To obtain $\dot{V}(x)$ and $V(x)$ for use as targets in the flight director, section 4.6, in real time for constant \dot{V} or \ddot{V} sections, solve Eqs. (B17) and (B24), respectively.

B.2.6.1 $\ddot{V} = \text{constant} \neq 0$:

Solve Eq. (B17) for Δt :

$$(\Delta t)^3 + \frac{3\dot{V}_j}{\ddot{V}}(\Delta t)^2 + \frac{6V_j}{\ddot{V}}(\Delta t) - \frac{6(\Delta x)}{1.69\ddot{V}} = 0 \quad \text{where } \Delta x = x - x_j$$

From ‘‘CRC Standard Math Tables’’ 11th edition, for cubic equations, let:

$$\Delta t = z - \frac{\dot{V}_j}{\ddot{V}}$$

Then:

$$z^3 + az + b = 0$$

where:

$$a = \frac{6V_j}{\ddot{V}} - 3\left(\frac{\dot{V}_j}{\ddot{V}}\right)^2$$

$$b = 2\left(\frac{\dot{V}_j}{\ddot{V}}\right)^3 - 6\left(\frac{\dot{V}_j V_j}{\ddot{V}^2}\right) - \frac{6(\Delta x)}{1.69\ddot{V}}$$

B.2.6.1.1 For $\dot{V} > 0$:

$$SR = \left(\frac{b^2}{4} + \frac{a^3}{27} \right)^{1/2}$$

$$\Delta t = -\frac{\dot{V}_j}{\dot{V}} + \left(-\frac{b}{2} + SR \right)^{1/3} + \left(-\frac{b}{2} - SR \right)^{1/3} \quad (\text{B26})$$

B.2.6.1.2 For $\dot{V} < 0$:

$$\phi = \cos^{-1} \left[\frac{-\frac{b}{2}}{\sqrt{\frac{(-a)^3}{27}}} \right]$$

$$\Delta t = -\frac{\dot{V}_j}{\dot{V}} + 2\sqrt{\frac{-a}{3}} \cos \left(\frac{\phi}{3} + \frac{4\pi}{3} \right) \quad (\text{B27})$$

Use Δt from Eqs. (B26) and (B27) in Eqs. (B15) and (B16) for $\dot{V}(x)$ and $V(x)$ target values for the flight director in section 4.6.

B.2.6.2 $\dot{V} = \text{constant}$, $\ddot{V} \equiv 0$:

From Eq. (B24):

$$V(x) = \left[V_j^2 + \frac{2\dot{V}(\Delta x)}{1.69} \right] \quad (\text{B28})$$

Use this value for the $V(x)$ target value for the flight director in section 4.6.

APPENDIX C: FLIGHTPATH, VELOCITY, AND LONGITUDINAL FLIGHT DIRECTOR DISPLAY DERIVATIONS

C.1 General

This appendix provides only the derivations for section 4.5, “Nominal Pitch, θ_N , and Thrust Lever Angle, δ_{TN} (or T_N)” as all other algorithm derivations are given either in section 4.0 or reference 1.

C.2 Rate of Change of Ground Speed, \dot{v}_{GA}

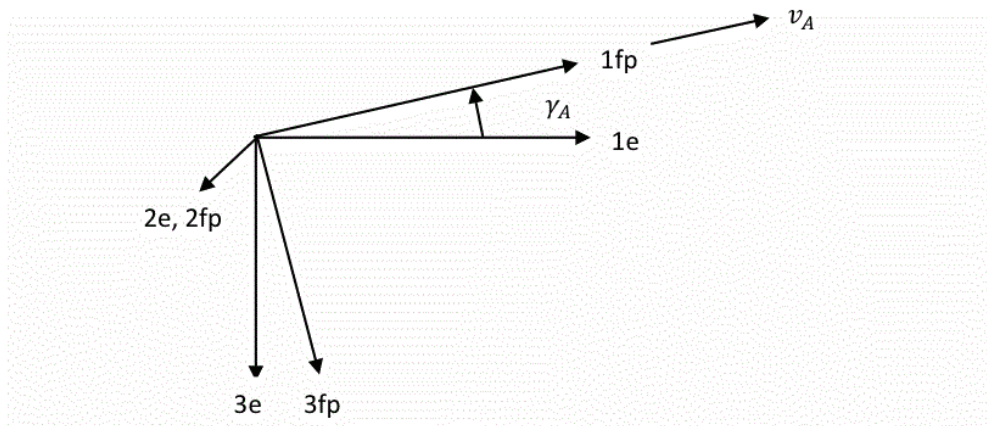
The vector equation of motion:

$$F_{ext}^{fp} + W^{fp} = m\dot{v}_G^{fp} = m(\dot{v}_G^{fp} + \Omega^{fp} \times v_G^{fp}) \quad \text{where } m = W/g \quad (C1)$$

in flightpath (fp) coordinates with respect to the air mass where:

F_{ext}^{fp}	external forces on the vehicle (lift, drag, thrust, etc.),	lb
v_G^{fp}	ground speed, the speed w.r.t. an Earth fixed coordinate frame in fp coordinates,	fps
\dot{v}_G^{fp}	rate of change of ground speed in inertial space,	fps ²
\dot{v}_G^{fp}	rate of change of ground speed in the fp coordinate frame,	fps ²
W	weight	lb
$\Omega^{fp} \times v_G^{fp}$	vector cross product of the rotational rate of the fp coordinates w.r.t. inertial space and ground speed,	fps ²

Define two right-hand coordinate frames, the Earth (e) and the flightpath (fp):



with:

$$A^{fp/e} = \begin{pmatrix} \cos \gamma_A & 0 & -\sin \gamma_A \\ 0 & 1 & 0 \\ \sin \gamma_A & 0 & \cos \gamma_A \end{pmatrix} \quad (C2)$$

where:

1fp is aligned along the true airspeed, v_A .

1e is aligned along the horizontal projection of the true airspeed, v_A , ψ degrees of heading from North (assuming zero sideslip).

1e-2e are in the ground plane.

γ_A is the angle (v_A flightpath angle) about 2e between the Earth, e, and fp coordinates.

$A^{fp/e}$ is the transform matrix between the e and fp coordinate frames.

Since W is aligned along the 3e axis:

$$W^{fp} = A^{fp/e} \begin{pmatrix} 0 \\ 0 \\ W \end{pmatrix} = \begin{pmatrix} -W \sin \gamma_A \\ 0 \\ W \cos \gamma_A \end{pmatrix} \quad (C3)$$

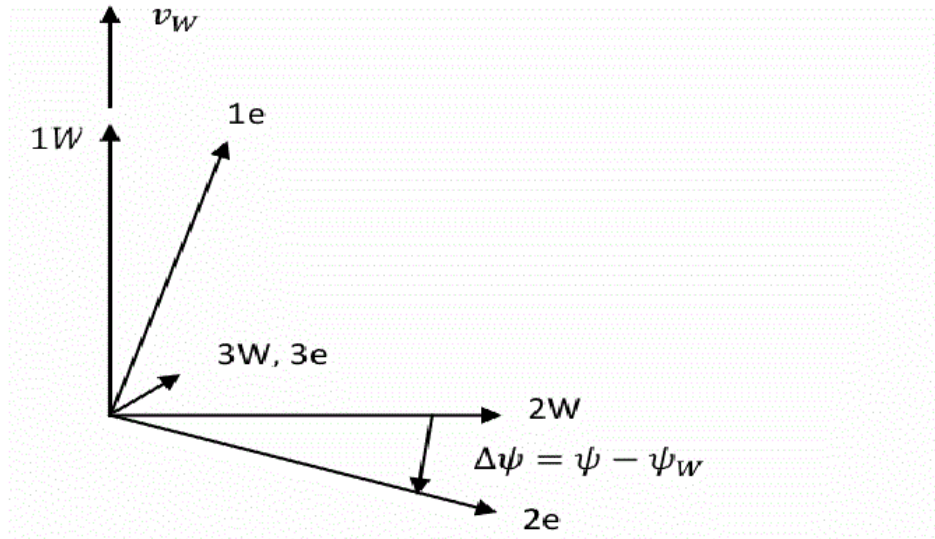
Since the rotational rate of the fp coordinates due to $\dot{\psi}$ is also aligned with the 3e axis and the rotational rate of the fp coordinates due to $\dot{\gamma}_A$ is aligned with the 2e and 2fp axis:

$$\Omega^{fp} = \begin{pmatrix} -\dot{\psi} \sin \gamma_A \\ \dot{\gamma}_A \\ \dot{\psi} \cos \gamma_A \end{pmatrix} \quad (C4)$$

Substituting Eqs. (C3) and (C4) into (C1), the vector component of the equation of motion along the true airspeed (flightpath 1fp axis) is:

$$\frac{F_{ext}^{1fp}}{W} = \sin \gamma_A + \frac{\dot{\gamma}_A^{1fp}}{g} + \frac{1}{g} (v_G^{3fp} \dot{\gamma}_A - v_G^{2fp} \dot{\psi} \cos \gamma_A) \quad (C5)$$

Define a wind coordinate frame, W:



with:

$$A^{e/W} = \begin{pmatrix} \cos \Delta\psi & \sin \Delta\psi & 0 \\ -\sin \Delta\psi & \cos \Delta\psi & 0 \\ 0 & 0 & 1 \end{pmatrix} \quad (C6)$$

where:

$$\Delta\psi = \psi - \psi_W$$

and:

1W is aligned along the direction of the wind vector, v_W , (assumed to be horizontal), ψ_W degrees from North.

$A^{e/W}$ is the transform matrix between the W and e coordinate frames.

For v_G^{fp} in Eq. (C5):

$$\begin{aligned} v_G^{fp} &= v_A^{fp} + v_W^{fp} = \begin{pmatrix} v_A \\ 0 \\ 0 \end{pmatrix} + A^{fp/e} A^{e/W} \begin{pmatrix} v_W \\ 0 \\ 0 \end{pmatrix} \\ &= \begin{pmatrix} v_A + v_W \cos \Delta\psi \cos \gamma_A \\ -v_W \sin \Delta\psi \\ v_W \cos \Delta\psi \sin \gamma_A \end{pmatrix} \end{aligned} \quad (C7)$$

Differentiate v_G^{1fp} in the fp frame to get \dot{v}_G^{1fp} and substitute it and v_G^{3fp} and v_G^{2fp} into Eq. (C5). Also assume $\sin \gamma_A \approx \gamma_A$ and $\cos \gamma_A \approx 1$:

$$\frac{F_{ext}^{1fp}}{W} = \gamma_A + \frac{1}{g} [\dot{v}_A + \dot{v}_W \cos(\psi - \psi_W) + v_W \dot{\psi}_W \sin(\psi - \psi_W)], \text{ rad} \quad (C8)$$

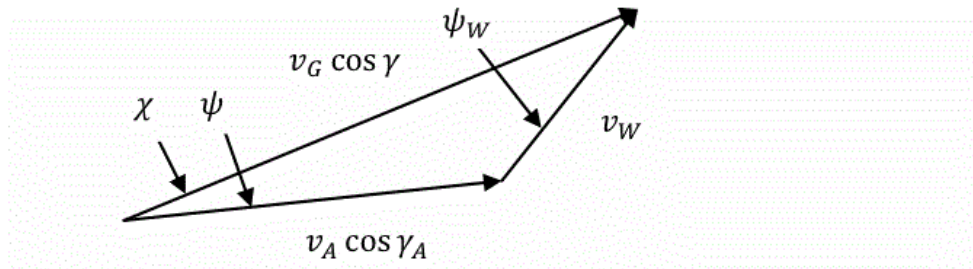
Let:

$$\dot{v}_{GA} = \dot{v}_A + \dot{v}_W \cos(\psi - \psi_W) + v_W \dot{\psi}_W \sin(\psi - \psi_W), \text{ fps}^2 \quad (C9)$$

This is Eq. (4.4) in section 4.5. Then Eq. (C8) becomes:

$$\frac{F_{ext}^{1fp}}{W} = \gamma_A + \frac{\dot{v}_{GA}}{g}, \text{ rad} \quad (C10)$$

Eq. (C9) for \dot{v}_{GA} requires knowing ψ , the heading in the presence of wind. In the 1e-2e plane:



where:

γ is the inertial flightpath angle, deg
 χ is the track angle, deg

Assume $\chi = \psi_t$, the nominal track angle from LNAV, and $\cos \gamma \approx \cos \gamma_A \approx 1$. Then from the law of sines:

$$\frac{v_A}{\sin(\psi_t - \psi_W)} = \frac{v_W}{\sin(\psi - \psi_t)} \quad (C11)$$

and Eq. (4.5) in section 4.5 becomes:

$$\psi = \psi_t + \sin^{-1} \left[\frac{v_W}{v_A} \sin(\psi_t - \psi_W) \right] \quad (C12)$$

Eq. (C9) also requires knowing \dot{v}_A , the rate of change of the true airspeed magnitude:

$$v_A = v_e \sigma^{-1/2}$$

$$\dot{v}_A = \dot{v}_e \sigma^{-1/2} - \frac{v_e}{2} \sigma^{-3/2} \frac{d\sigma}{dh} \frac{dh}{dt}$$

Assume:

$$\sigma \approx e^{-h/H}, \quad H = 26,000 \text{ ft}$$

Then:

$$\frac{d\sigma}{dh} = -\frac{\sigma}{H}$$

since:

$$\frac{dh}{dt} = v_G \tan \gamma$$

$$\dot{v}_A = \sigma^{-1/2} \left(\dot{v}_e + \frac{v_e v_G}{2H} \tan \gamma \right), \quad \text{fps}^2 \quad (C13)$$

where:

σ	atmospheric density ratio	
v_e	equivalent airspeed magnitude from VNAV,	fps
\dot{v}_e	rate of change of equivalent airspeed magnitude,	fps ²

Eq. (C13) is Eq. (4.6) in section 4.5.

C.3 Gamma, $\gamma_{\gamma V}$, for Determining Nominal Pitch, θ_N , and Thrust Lever Angle, δ_{TN} (or T_N) from the γ/V Diagrams

From the discussion in section 3.1.3 and Eq. (C10) and since in Eq. (C10):

$$\gamma_A \approx \frac{\dot{h}}{v_A} = \frac{\dot{h}}{v_G} \frac{v_G}{v_A} = \gamma \frac{v_G}{v_A}$$

the gamma to enter the γ/V diagrams is:

$$\gamma_{\gamma V} = \gamma \frac{v_G}{v_A} + \frac{180}{\pi} \frac{\dot{v}_{GA}}{g}, \quad \text{deg} \quad (C14)$$

This is Eq. (4.3) in section 4.5.

REFERENCES

1. Hardy, G.H.: Pursuit Display Review and Extension to a Civil Tilt Rotor Flight Director. AIAA-2002-4925, Aug. 2002.
2. Moralez, et al.: In-Flight Assessment of a Pursuit Guidance Display Format for Manually Flown Precision Instrument Approaches. AHS 60th Annual Forum, June 2004.
3. Hynes, C.S.; Franklin, J.A.; Hardy, G.H.; Martin, J.L.; and Innis, R.C.: Flight Evaluation of Pursuit Displays for Precision Approach of Powered-Lift Aircraft. AIAA J. Guidance and Control, July–Aug. 1989, pp. 521–529.
4. Merrick, V.K.; Farris, G.G.; and Vanags, A.A.: A Head Up Display for Application to V/STOL Aircraft and Landing. NASA TM 102216, Jan. 1990.
5. Merrick, V.K.: Some VTOL Head-Up Display Drive-Law Problems and Solutions. NASA TM 104027, Nov. 1993.
6. Merrick, V.K.; and Jeske, J.A.: Flightpath Synthesis and HUD Scaling for V/STOL Terminal Area Operations. NASA TM 110348, April 1995.
7. Franklin, J.A.; Stortz, M.W.; Borchers, P.F.; and Moralez III, E.: Flight Evaluations of Advanced Controls and Displays for Transition and Landing on the NASA V/STOL Systems Research Aircraft. NASA TP 3607, April 1996.
8. Bray, R.S.: A Head-Up Display Format for Application to Transport Aircraft Approach and Landing. NASA TM 81199, July 1980.
9. Williams, E.: Aviation Formulary V1.45. <http://williams.best.vwh.net/avform.htm>, 2010.